JGR Biogeosciences

RESEARCH ARTICLE
10.1029/2023JG007583

Hydrology Controls Dissolved Organic Carbon and Nitrogen Export and Post-Storm Recovery in Two Arctic Headwaters

Arial J. Shogren[1,2], Jay P. Zarnetske[2], Benjamin W. Abbott[3], Amelia L. Grose[2], Abigail F. Rec[4], Jansen Nipko[3], Chao Song[2,5], Jonathan A. O'Donnell[6], and William B. Bowden[4]

[1]Biological Sciences Department, The University of Alabama, Tuscaloosa, AL, USA, [2]Michigan State University Department of Earth and Environmental Sciences, East Lansing, MI, USA, [3]Department of Plant and Wildlife Sciences, Brigham Young University, Provo, UT, USA, [4]Rubenstein School of the Environment and Natural Resources, University of Vermont, Burlington, VT, USA, [5]State Key Laboratory of Herbage Improvement and Grassland Agro-ecosystems and College of Ecology, Lanzhou University, Lanzhou, China, [6]National Parks Service, Arctic Network, Anchorage, AK, USA

Abstract Climate change is rapidly altering hydrological processes and consequently the structure and functioning of Arctic ecosystems. Predicting how these alterations will shape biogeochemical responses in rivers remains a major challenge. We measured [C]arbon and [N]itrogen concentrations continuously from two Arctic watersheds capturing a wide range of flow conditions to assess understudied event-scale C and N concentration-discharge (*C*-*Q*) behavior and post-event recovery of stoichiometric conditions. The watersheds represent low-gradient, tundra landscapes typical of the eastern Brooks Range on the North Slope of Alaska and are part of the Arctic Long-Term Ecological Research sites: the Kuparuk River and Oksrukuyik Creek. In both watersheds, we deployed high-frequency optical sensors to measure dissolved organic carbon (DOC), nitrate (NO_3^-), and total dissolved nitrogen (TDN) for five consecutive thaw seasons (2017–2021). Our analyses revealed a lag in DOC:NO_3^- stoichiometric recovery after a hydrologic perturbation: while DOC was consistently elevated after high flows, NO_3^- diluted during rainfall events and consequently, recovery in post-event concentration was delayed. Conversely, the co-enrichment of TDN at high flows, even in watersheds with relatively high N-demand, represents a potential "leak" of hydrologically available organic N to downstream ecosystems. Our use of high-frequency, long-term optical sensors provides an improved method to estimate carbon and nutrient budgets and stoichiometric recovery behavior across event and seasonal timescales, enabling new insights and conceptualizations of a changing Arctic, such as assessing ecosystem disturbance and recovery across multiple timescales.

Plain Language Summary The Arctic is one of the first regions to experience the impacts of climate change and is already experiencing rapid changes to the water cycle, seasonality, and permafrost state. These changes can be expressed in the chemistry observed in a river network, and ecosystem-scale responses to change are integrated at a watershed outlet. With this study, we leveraged 5 years of high-frequency data collected from two Arctic headwaters to observe how these watersheds respond to hydrologic disturbance. Overall, we found that at the event-scale, Arctic rivers are responsive to precipitation events, where carbon (C) increases and reactive nitrogen (N) as nitrate (NO_3^-), is diluted in tandem when a storm event occurs. We also found that after the peak of the storm event, there is a difference in recovery rates for C and N that indicate storm events represent a hydrologic and biogeochemical disturbance. Overall, our findings are important for documenting hydrologic responses to a changing Arctic.

Key Points:

- In both watersheds, we found consistent divergent responses of dissolved organic carbon (DOC) and nitrate to hydrologic disturbance
- DOC:TDN responded convergently during storms, suggesting a large pool of hydrologically available organic matter in tundra landscapes
- The use of high-frequency optical sensor data provides an improved method to estimate carbon and nutrient behavior at the event timescale

Supporting Information:

Supporting Information may be found in the online version of this article.

Correspondence to:

A. J. Shogren,
arialshogren@gmail.com

Citation:

Shogren, A. J., Zarnetske, J. P., Abbott, B. W., Grose, A. L., Rec, A. F., Nipko, J., et al. (2024). Hydrology controls dissolved organic carbon and nitrogen export and post-storm recovery in two Arctic headwaters. *Journal of Geophysical Research: Biogeosciences*, *129*, e2023JG007583. https://doi.org/10.1029/2023JG007583

Received 19 MAY 2023
Accepted 4 DEC 2023

Author Contributions:

Conceptualization: Arial J. Shogren, Jay P. Zarnetske, Benjamin W. Abbott, Amelia L. Grose, Chao Song, Jonathan A. O'Donnell, William B. Bowden
Data curation: Arial J. Shogren
Formal analysis: Arial J. Shogren
Funding acquisition: Arial J. Shogren, Jay P. Zarnetske, Benjamin W. Abbott, Jonathan A. O'Donnell, William B. Bowden

1. Introduction

Climate change is profoundly reshaping Arctic landscapes, resulting in antagonistic and synergistic effects on ecosystem structure and function (Bring et al., 2016; Prowse et al., 2015), redefining the complex interactions between terrestrial and aquatic ecosystems (Harms et al., 2016). Concurrent shifts in terrestrial vegetation cover and productivity (Loranty & Goetz, 2012; Myers-Smith et al., 2011) and a marked increase in the length of the growing seasons are leading to changes in terrestrial and soil resource pools (Drake et al., 2018; Ebel et al., 2019; Ernakovich et al., 2014; Schuur et al., 2022). Further, the combination of altered hydrologic regimes (Beel et al., 2020; Bintanja & Andry, 2017; Dery et al., 2005; Dou et al., 2022; McCrystall et al., 2021), amplified permafrost degradation (Abbott et al., 2015; Kokelj & Jorgenson, 2013; Lafreniere & Lamoureux, 2013; Vonk et al., 2015; Walvoord & Kurylyk, 2016), and increased potential for lateral and longitudinal transfer

Investigation: Arial J. Shogren, Amelia L. Grose, Abigail F. Rec, Jansen Nipko, Chao Song, Jonathan A. O'Donnell
Methodology: Arial J. Shogren
Project Administration: Benjamin W. Abbott
Resources: Arial J. Shogren, Jay P. Zarnetske, Benjamin W. Abbott, Chao Song, Jonathan A. O'Donnell, William B. Bowden
Validation: Arial J. Shogren
Visualization: Arial J. Shogren
Writing – original draft: Arial J. Shogren
Writing – review & editing: Arial J. Shogren, Jay P. Zarnetske, Benjamin W. Abbott, Amelia L. Grose, Abigail F. Rec, Jansen Nipko, Chao Song, Jonathan A. O'Donnell, William B. Bowden

of hydrologically available [C]arbon and [N]itrogen (Harms & Jones, 2012; Lafrenière & Lamoureux, 2019; Wickland et al., 2018) are fundamentally changing solute fluxes in Arctic rivers (Frey & McClelland, 2009; McClelland et al., 2007; Tank et al., 2012). In addition, there is growing recognition that landscape characteristics lead to unique watershed biogeochemical responses to thaw (Connolly et al., 2018; Harms et al., 2016; Tank et al., 2020), as landscape characteristics interact with hydrologic and seasonal factors to ultimately control rates of C and N export (Vonk et al., 2019). Still, changes in lateral C and N flux are one of the largest sources of uncertainty in modeling net ecosystem biogeochemical balance of permafrost zones (Abbott et al., 2021; Drake et al., 2018; McGuire et al., 2018), and are of great interest to constrain Earth-system models that predict global response to biogeochemical change (Fan et al., 2019; Kicklighter et al., 2013; Treharne et al., 2022).

While systemic changes to Arctic ecosystems may have both antagonistic and synergistic effects on ecosystem structure and function, they manifest as alterations in water-mediated fluxes (Saros et al., 2022; Shogren et al., 2021; Tank et al., 2020; Vonk et al., 2019). The expression of changing river chemistry at the event scale can reflect the dominant sources and pathways of material as they are transferred from terrestrial zones to the stream channel (Godsey et al., 2009, 2019; Moatar et al., 2017). While this perspective has been widely applied across temperate regions, the combination of technological advancements and increasing interest in capturing processes that control the transport of material across the terrestrial-aquatic nexus have been recently applied in permafrost-underlain watersheds (Conroy et al., 2022; Khamis et al., 2021; Shogren et al., 2021; Webster et al., 2021). Namely, the application of concentration-discharge (hereafter *C-Q*) metrics from high-frequency time-series data has revealed the dominant landscape and seasonal controls on lateral C and N exports in Arctic and Boreal watersheds (Khamis et al., 2021; Shogren et al., 2021; Webster et al., 2021). For example, Shogren et al. (2021) leveraged high-frequency monitoring efforts to quantify event-scale *C-Q* responses for dissolved organic C (DOC) and nitrate (NO_3^-) from Arctic headwater watersheds. The study found that landscape attributes such as slope, the presence of stream-lake chains, and vegetation were the dominant controls of DOC and NO_3^- *C-Q* responses during rainfall events, while the season was not a significant predictor of *C-Q* responses (Shogren et al., 2021). Such studies underscore that *C-Q* responses reveal the drivers of storm-driven export in Arctic watersheds, especially given rapid changes in the timing and magnitude of precipitation events that transport material and reactive nutrients from land to water (Beel et al., 2020; McCrystall et al., 2021).

Across regions, most *C-Q* studies describe the responses of individual constituents, such as DOC, dissolved inorganic nitrogen (DIN), or reactive phosphorus in temperate rivers (Fazekas et al., 2020; Khamis et al., 2021; Raymond & Saiers, 2010; Vaughan et al., 2017; Wagner et al., 2019; Zarnetske et al., 2018), as well as in permafrost-influenced landscapes (Shogren et al., 2021; Webster et al., 2021). Efforts to capture multi-solute response across seasons (Kincaid et al., 2020), land use and land cover (Fazekas et al., 2021; Wymore et al., 2021), and antecedent hydrologic conditions (Gorski & Zimmer, 2021; Ledesma et al., 2022) have significantly advanced applications of the *C-Q* method by acknowledging that the transport of reactive solutes during storm events is inherently linked with the availability of other solutes and should be assessed in unison (Ledesma et al., 2022; Marcé et al., 2018; Wymore et al., 2021). For example, many studies in temperate regions recognize that the instream transport and transformation of C and N are inherently coupled (Plont et al., 2020), both directly through processes such as denitrification and assimilatory N processes (Burgin & Hamilton, 2007; Helton et al., 2015; Rodríguez-Cardona et al., 2020) and indirectly through stoichiometric constraints (Frei et al., 2020; Taylor & Townsend, 2010). Differences in *C-Q* responses between C and N may create stoichiometric shifts in rivers and could consequently alter rates of C and N transformation. Only through joint exploration of C and N *C-Q* responses can we elucidate how their couple biogeochemical cycles may shift. Specifically in the context of high-latitude ecosystems, assessing the coupled C and N dynamics in Arctic rivers could enhance our understanding of ongoing ecological changes, including more incorporation of ecosystem disturbance and resilience theories (Gunderson, 2000; Holling, 1973).

While past work (Shogren et al., 2021) focused on the role of landscape characteristics and season on single-solute DOC and NO_3 *C-Q* responses in high-latitude watersheds, our objective with this study was to expand on the interpretation of *C-Q* responses by considering multi-solute behavior and recovery at the event-scale. Our guiding questions were: (a) *How do paired C and N C-Q responses vary across inorganic and organic dissolved N forms?* and (b) *How do these responses differ across two Arctic watersheds with different ecological characteristics?* To answer these questions, we re-investigated several years of high-frequency chemistry data from optical water quality sensors (2017–2019, Zarnetske et al., 2020a, 2020b), adding two additional years of record (Shogren et al., 2023a, 2023b). In addition, we calibrated the high-frequency spectral data to include novel estimates of TDN, in addition to DOC and NO_3. Together, these data allowed us to describe the temporal variability in coupled

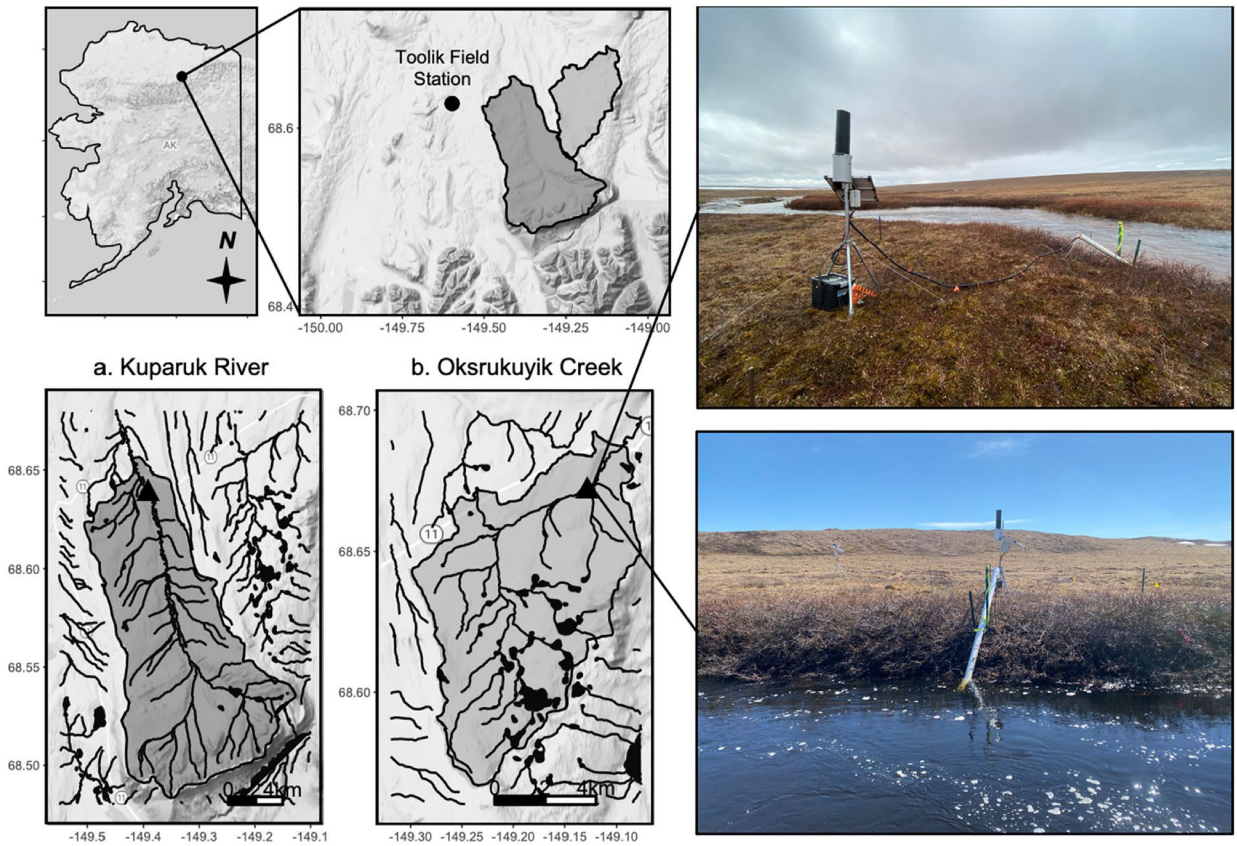

Figure 1. Map of the state of Alaska, USA, highlighting an inset of the region near Toolik Field Station on the North Slope. Map of our study watersheds associated with Toolik Field Station in Northern Alaska, the Upper Kuparuk River (a), and Oksrukuyik Creek (b). Sensor locations are noted by a small triangle. Scale bar represents 2 km increments. Picture of the s::can sensor deployments in Oksrukuyik Creek, looking upstream (top) and from the other side of the river (bottom).

C and N exports in two permafrost-underlain Arctic watersheds: the Upper Kuparuk River (low lake density) and Oksrukuyik Creek (high lake density) (Figure 1). Across both watersheds, we expected that event-driven export would result in divergent *C-Q* responses resulting from rapid flushing of hydrologically available and abundant DOC and simultaneous rapid dilution of NO_3^- (Harms & Jones, 2012; Khosh et al., 2017). Conversely, we predicted convergent *C-Q* exports of DOC and TDN, given the high organic N content of the dissolved organic matter pool which hydrologically connected and co-mobilized at the event scale. In addition to reporting the event-scale *C-Q* responses, we used the high-frequency data to explore post-peak recovery of C and N. Thus, we developed a competing hypothesis for comparing *C-Q* recovery across watersheds: that we would observe more change and slower recovery in the Oksrukuyik than in the Kuparuk given greater residence time within the lake chains. Alternatively, we hypothesized that we would note less change and faster recovery in the lake-dominated watershed because of greater in-network processing capacity and therefore "buffered" *C-Q* responses observed at the watershed outlet relative to the Kuparuk.

2. Materials and Methods

2.1. Site Description

Our study watersheds, the Upper Kuparuk River and Oksrukuyik Creek (Figure 1), are part of the Arctic Long-Term Ecological Research (LTER) site based out of Toolik Field Station in the foothills of the Brooks Range on the North Slope of Alaska, USA (60° 38′N, −149° 36.4′W, elevation 720 m) (Hobbie & Kling, 2014). We chose these watersheds as they encompass the dominant tundra vegetation types, permafrost characteristics, and hydrologic conditions typical of the North Slope (Table 1).

The Upper Kuparuk River watershed (68°38′47″, −149°24′34″, Figure 1a) is a long-term monitoring site for the Arctic LTER, used as a site for ecological study and monitoring since 1979. The Kuparuk is a meandering braided

Table 1
Arctic Watershed Characteristics and Monitoring Dates for the 2017–2021 Sensor Deployments in the Kuparuk River and Oksrukuyik Creek

Site	Kuparuk River	Oksrukuyik Creek
Total Drainage Area (km^2)	92.5	72.6
Mean Slope (°)	3.1	3.2
Mean Elevation (m)	988	862
Geologic Setting	Sagavanirktok Old Glaciated Uplands	Sagavanirktok Young Glaciated Valleys
Hydrologic Setting	Continuous permafrost	Continuous permafrost
Primary landscape classification	Wet acidic tundra	Wet acidic tundra
Surface Area of Lakes (km^2)	0.59	3.3
% Area Covered by Lake	0.65%	4.50%
Stream Strahler Order	4th	3rd
Mean Normalized Difference Vegetation Index (NDVI) in June and August	4324 ± 522 (June) 4535 ± 1022 (August)	4789 ± 1106 (June) 4535 ± 1022 (August)
Monitoring Dates		
2017	6/2–9/23	6/2–8/14
2018	7/3–9/3	7/4–9/3
2019	6/16–8/10	6/16–9/10
2020	6/27–9/17	7/1–9/17
2021	6/9–9/1	5/25–9/1

stream network flowing through dominantly wet acidic tundra vegetation cover, including tussock (46%), shrubby birches and willows (25%), and sedges (14%) (Shogren et al., 2022). Its underlying geology is composed of glacial alluvial and outwash deposits from the Sagavanirktok glaciation in the late Pleistocene (Hamilton, 2003; Walker & Raynolds, 2017). The watershed is underlain by continuous permafrost, with soils made of colluvial deposits and organic matter (Walker & Maier, 2008). Though annual discharge is dominated by the spring freshet (Finlay et al., 2006; Townsend-Small et al., 2011), flow generation in this watershed is highly responsive to precipitation events (McNamara et al., 1998).

The Oksrukuyik Creek watershed (68°41′12″, −149°05′50″, Figure 1b) is both an Arctic LTER watershed and an established National Ecological Observatory Network monitoring site. Oksrukuyik Creek is considered a clear-water, low-gradient stream meandering through primarily tundra landscape, with a series of lake chains in the headwaters (Shogren et al., 2019, 2022). Vegetation cover in Oksrukuyik Creek watershed is dominated by tussock tundra (58%), sedge (24%), birch/willow shrub tundra (11%), and open water (4%) (Shogren et al., 2022). The watershed sits on glacial and alluvial deposits from the Itkillik (phase I) glaciation (Hamilton, 2003; Walker & Raynolds, 2017). The entire watershed is underlain by continuous permafrost, though taliks can form under lakes and stream channels. The Oksrukuyik Creek watershed drains a cluster of lakes at its headwaters and flows into the Sagavanirktok River.

2.2. High-Frequency Sensor Deployment and Data Collection

We collected high-frequency data of stream flow and solute concentrations from the study watersheds during most of the thaw season, from early June through early September, for five consecutive years (2017–2021; exact dates noted in Table 1 and Figure 2). In each watershed, we estimated discharge using co-located, atmospherically compensated pressure transducers (Onset HOBO, Bourne Massachusetts, USA) that recorded water depth (stage, *m*) at 10-min intervals. We converted these stage data to continuous discharge using regular velocity-area calculations from weekly field measurements (Perumal et al., 2007; Turnipseed & Sauer, 2010) (Figure 2). Concurrently, we measured water chemistry in 15-min intervals using submersible UV-visible spectrophotometers (s::scan Messtechnik GmbH, Vienna, Austria), which were co-located with the pressure transducers. The spectrophotometers measure light absorbance at wavelengths from 200 through 750 nm normalized spectra through a 35-mm

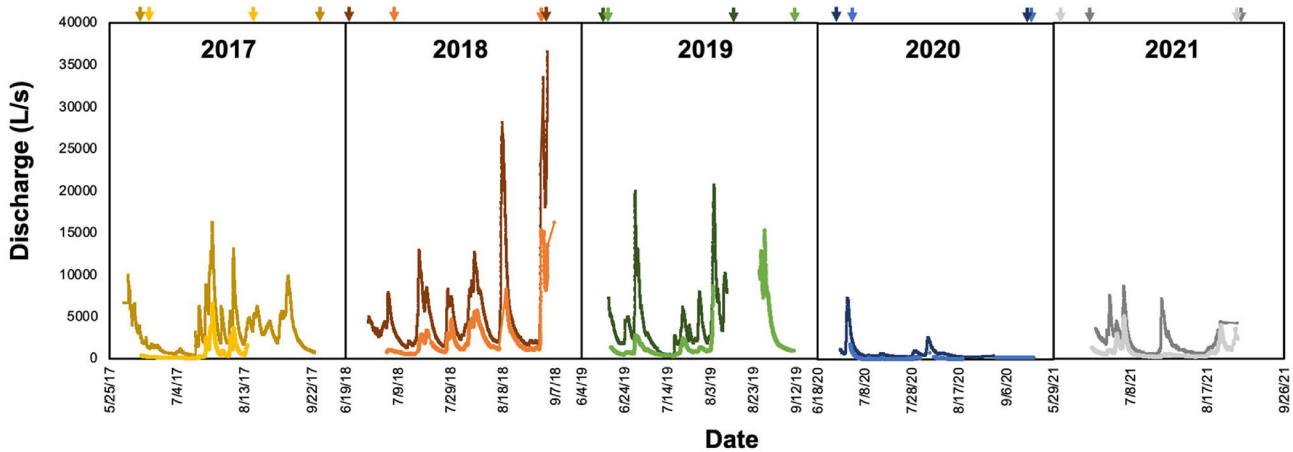

Figure 2. Annual hydrographs of our study watersheds associated with Toolik Field Station in Northern Alaska, the Kuparuk River (darker color) and Oksrukuyik Creek (lighter color) from 2017 to 2021. Arrows correspond to s::can and PT logger deployment dates for the Kuparuk (darker arrow) and Oksrukuyik (lighter arrow) for each year. Please note the differences in the range of deployment dates (*x-axes*) for each year and watershed, which are further described in Table 1.

optical path (Edwards et al., 2001; Ruhala & Zarnetske, 2017). In the minute prior to collecting the absorbance reading, the spectrophotometers automatically cleaned their lenses with a rotating brush. We also manually cleaned the sensor lens every 2–3 weeks. We housed the sensors in protective PVC tubing anchored with fence posts on the streambed. While every effort was made to deploy the sensors and PT loggers as early as possible, field logistics and safety concerns often limited deployment during freshet conditions. In the Kuparuk and Oksrukuyik, the freshet generally begins in late-May, and our sensor deployments are typically only feasible starting in early to mid June. The sensor deployment dates varied slightly each year, depending on weather, river deicing, and flow conditions, but they encompassed most of the flow season after the freshet and ice-off conditions, from early to mid-June through late-August or September (Table 1). Therefore, our results are only representative of early to late-season storm events, and do not fully characterize the freshet or snowmelt period in the Kuparuk or Oksrukuyik.

In each watershed, we collected biweekly grab samples of stream water at the sensor sites to analyze DOC, NO_3^-, and TDN concentrations in the laboratory to allow site-specific calibration of the absorbance spectra (Ruhala & Zarnetske, 2017). We filtered each field sample using either 0.7-µm glass fiber filters (Whatman GF/F, 2017-2020, samples acidified to 0.1 M with HCl) or 0.2-µm cellulose acetate filters (Sterilite CA, 2021, samples not acidified) into clean HDPE bottles. For all years, we refrigerated (DOC, TDN) or froze (NO_3^-) filtered water samples until prompt laboratory analysis. We measured DOC and TDN on a Shimadzu TOC-L analyzer with a TN module using a combustion catalytic method. We analyzed NO_3^- on a QuickChem Lachat analyzer (2017 samples) or a SEAL AA3 segmented flow analyzer (2018–2021 samples).

With the lab-measured concentrations, we used a partial least squares regression (PLSR) variable-selection approach to generate robust calibration relationships between turbidity-corrected UV-visible absorbance spectra and observed grab samples for DOC, NO_3^-, and TDN independently (Etheridge et al., 2014; Vaughan et al., 2018). These solutes impact the absorbance of light at various wavelengths across the UV-vis spectrum (Sakamoto et al., 2009), resulting in high dimensionality between the light absorbance spectra relative to predicting the solute concentration of interest. A PLSR approach is advantageous relative to a simple linear model of predicted versus observed concentrations because it reduces this dimensionality by condensing many uncorrelated components into a multi-variate model capable of predicting the solute of interest (Etheridge et al., 2014). Briefly, to generate the predicted time-series record, we established independent PLSR calibration models for each solute (DOC, NO_3^-, and TDN) for each watershed and year from the observed grab sample concentrations relative to the sensor-generated absorbance spectra at the closest sampling time point. We used our initial PLSR-predicted concentration as our training calibration model. For our study, this process resulted in 30 unique PLSR models (see Figures S1–S5 in Supporting Information S1 for comparison between observed versus PLSR-predicted concentrations). For each solute, watershed, and year, we then generated training data sets, where we applied the PLSR-training model to a random subset (85%) of the entire season's spectral data. The training model was then

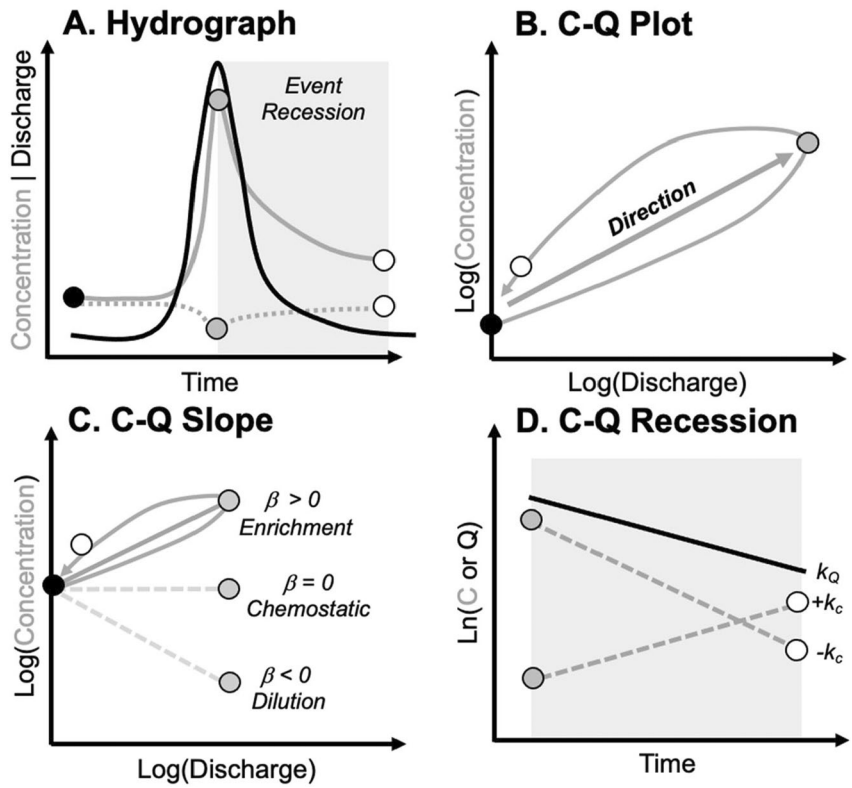

Figure 3. (a) A typical storm event monitoring pre-event (black point), peak flow (gray point), and post-event river concentrations of an enriching (solid gray line) or diluting (dashed gray line) solute as discharge (Q, solid black line) changes over time. (b) The biplot of log-log concentration-discharge (C-Q) relationship (gray line) shows the direction of the entire storm event relationship. (c) The slope of the power-law C-Q slope (β) denotes the relationship between the entire chemograph as enriching ($\beta > 0$), chemostatic ($\beta \sim 0$), or diluting ($\beta < 0$). (d) Event recession constant, k, over the recession period. A positive k indicates an increase in concentration since peak flow, while a negative k indicates a decrease in concentration post-peak.

used to predict a validation set using the remaining 15% of spectral data. We fit linear correlations between the predicted training and validation sets and the lab-measured values to establish the calibration model's goodness of fit (as in Vaughan et al., 2018). Once each PLSR model was validated, we generated the predicted continuous time-series record of concentration. We used the packages *pls* (Mevik & Wehrens, 2007; R Core Team, 2014) and tools from *plantspec* (Griffith & Anderson, 2019) to fit season and watershed-specific PLSR calibration models in R 4.0.3 (R Core Team, 2014).

2.3. Analysis of Concentration-Discharge Relationships and Recession Constants

To assess C-Q responses in our watersheds, we used an event-based approach. We used the *hydrostats* R package (Bond, 2019) to first identify putative flow events in the continuous discharge data and then differentiate baseflow and stormflow using a Lyne-Hollick filter (Ladson et al., 2013) (Figure 3a). Using this filter on the discharge record, we considered a storm to be an "event" when discharge increased at least 10% above baseflow conditions. After delineating each storm event based on this procedure, we further classified prolonged events that had multiple peaks as embedded, separate events using each peak minimum to separate events into individual events for further analysis. In the Kuparuk and Oksrukuyik, respectively, we captured 13 and 8 (2017); 9 and 8 (2018); 9 and 6 (2019), 6 and 6 (2020), and 6 and 4 (2021) events.

We first determined the event-scale C-Q relationship using a power law function ($C = \alpha Q^{\beta}$), where α is a scaling factor and β is the exponent representing the slope of the log-transformed C-Q response (Godsey et al., 2009) (Figures 3b and 3c). The C-Q slope (β) leverages data from the entire event hydrograph, thus capturing the direction and pattern of water chemistry across the rising and falling limb of the storm. To describe variations

in solute concentration with discharge, we classified *C-Q* responses as enriching ($\beta > 0$), constant ($\beta = 0$), or diluting ($\beta < 0$). To determine the dominant source of variability inherent in the *C-Q* response, we calculated the ratio of the coefficient of variation of concentration relative to discharge (CV_C/CV_Q) for each event (Thompson et al., 2011; Wymore et al., 2021). A ratio where $CV_C/CV_Q < 1$ reflects little variability in *C* relative to *Q*, where variation in exports is driven primarily by variations in flow. A ratio of $CV_C/CV_Q > 1$ indicates greater variability in C than *Q*, representing conditions where variability is driven predominantly by biogeochemical processes within the watershed, the timing of inputs, or the spatial variability in source pools.

We then compared the *C-Q* slopes of two solutes of interest to investigate how C and N are co-exported during storm events. We therefore plotted all event slopes of C versus those of N, resulting in biplots that enable classification of event-scale *C-Q* patterns as *convergent* or *divergent* export behaviors based on the placement of an event across four quadrants. While the terms synchrony and asynchrony have been similarly used to categorize *C-Q* patterns (Wymore et al., 2021), in the present study, the terms convergent and divergent are used to signify the coherence of *C-Q* behavior of C relative to N. We classified each event by cataloging them into four quadrants that describe the emergent patterns for paired C and N as follows: *quadrant 1*, both C and N *C-Q* responses are convergently enriching ($\beta > 0$); *quadrant 2*, divergent *C-Q* behavior where N is enriching ($\beta > 0$) while C is diluting ($\beta < 0$); *quadrant 3*, both C and N *C-Q* responses are convergently diluted ($\beta < 0$); and *quadrant 4*, divergent *C-Q* behavior where N is diluted ($\beta < 0$) while C is enriched ($\beta > 0$). We considered points within quadrants 1 and 3 to exhibit convergent C and N export behavior, while we defined quadrants 2 and 4 as divergent *C-Q* behavior.

Second, to assess the biogeochemical recovery after each storm event, we estimated nutrient recession constants, a parameter describing how fast solute concentrations fall back to pre-storm levels, for DOC, NO_3^-, and TDN concentrations (Figure 3d) (Knapp et al., 2020). This relationship between solute concentrations and streamflow during the hydrograph recession can be especially informative about transport processes from shallow water sources (Inamdar et al., 2006). Using the same delineated storms from the *C-Q* analysis, we selected data from the storm discharge peak of the event until 95% of the hydrograph recession to baseflow or until the event was cut off by the start of a subsequent event. We estimated concentration recession constants (k_c, d^{-1}) as the rate constant in an exponential decay $C(t) = C_o e^{-kt}$ (Brutsaert & Nieber, 1977). Conceptually, the concentration recession constant captures the subsequent "recovery" after the peak of a storm event (Knapp et al., 2020). A positive value of k_c indicates that concentration increased after peak flow, while a negative value suggests concentration decreased after peak flow (Figure 3d). We did the same for the hydrograph recession (k_Q, d^{-1}), using equation $Q(t) = Q_o e^{-kt}$.

2.4. Statistical Analyses

To explore differences across our two watersheds and monitoring years, we used two-way analysis of variances (ANOVAs) to assess differences in *C-Q* responses (β, CV_C/CV_Q, k_c), testing for an interaction between watershed and year. We used Shapiro-Wilk tests to test our data set for Normality and checked for heteroscedasticity using residual plots. Our data were normally distributed ($a > 0.05$). When we observed significant differences in the two-way ANOVAs, we used Tukey's post-hoc tests to determine differences in watershed or annual means. We compared recession *C-Q* β and recession constants (k_C) of C and N using simple linear regression models. We conducted all statistical tests using R (Version 4.0.3).

3. Data

The data set generated for both watersheds included timeseries of water chemistry (in mg/L) and discharge (L/s) (Zarnetske et al., 2020a, 2020b). These datas ets were used to generate *C-Q* metrics (Section 2.3).

4. Results

4.1. Event-Scale Metrics

We first report *C-Q* responses as β for DOC, NO_3^-, and TDN independently for each watershed and monitoring year in Figures 4a–4c. Across both study watersheds, we found a consistent pattern of enrichment ($\beta > 0$) for DOC and TDN in both watersheds and dilution ($\beta < 0$) for NO_3^- (Figure 4). We observed no statistical differences for β between watersheds or across years for NO_3^- ($F_{4, 58} = 1.895$, $p = 0.124$, Figure S6 in Supporting Information S1). However, there were differences in DOC β between watersheds (ANOVA; $F_{1, 62} = 4.612$, $p = 0.036$),

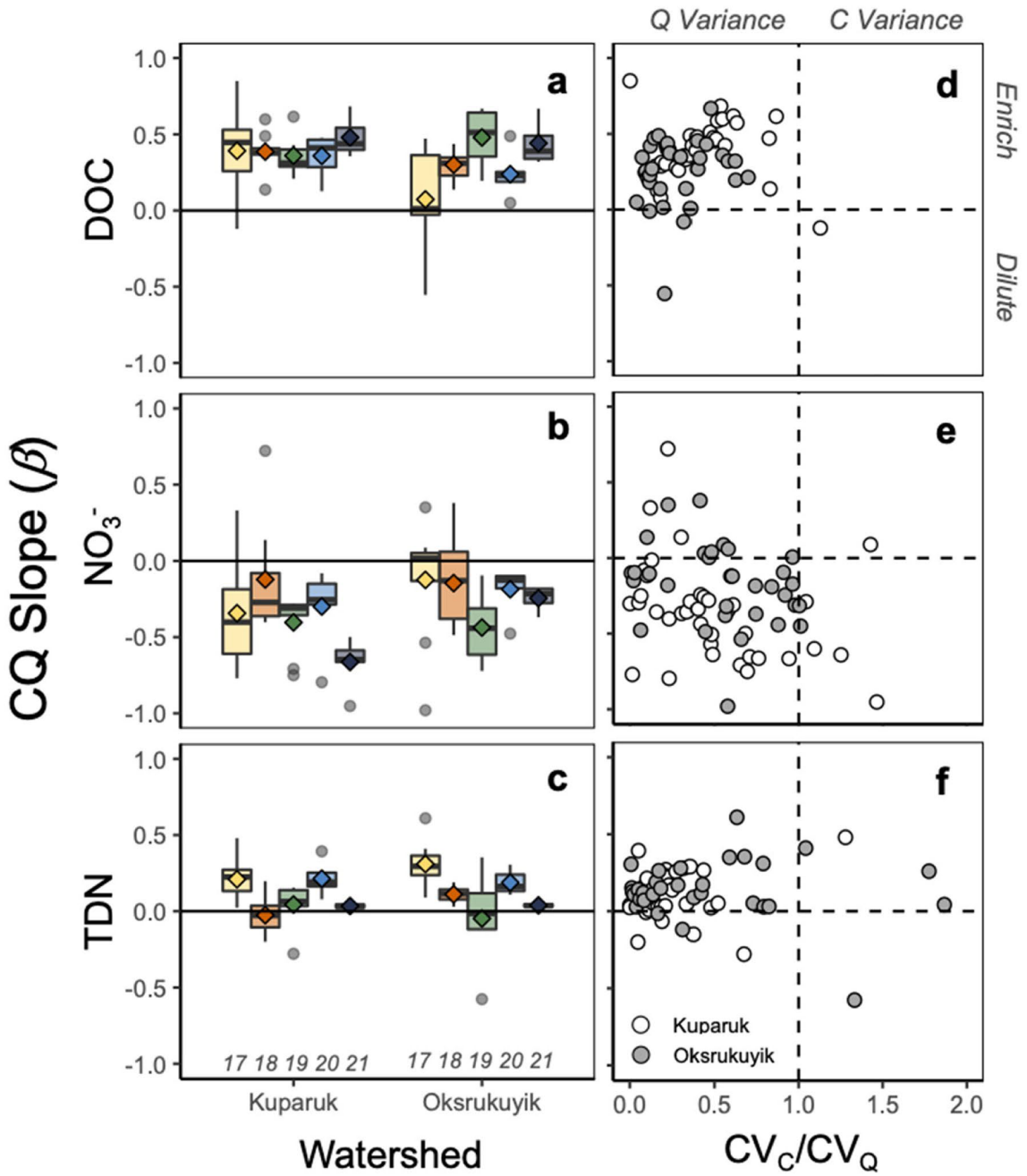

Figure 4. Boxplots of *C-Q* slope (as β) for (a) Dissolved Organic Carbon (DOC), (b) Nitrate (NO_3^-), and (c) Total Dissolved Nitrogen (TDN) for the Kuparuk and Oksrukuyik watersheds from 2017 (yellow), 2018 (orange), 2019 (green), 2020 (blue), and 2021 (gray). We report annual mean and median *C-Q* β reported as a point and horizontal bar, respectively. Note the horizontal reference line at $y = 0$, where $\beta > 0$ indicates solute enrichment and $\beta < 0$ suggests solute dilution during a high flow event. We also include a comparison of the CV_C/CV_Q ratio for (d) DOC, (e) NO_3^-, and (f) TDN for the Kuparuk (white circles) and Oksrukuyik (gray circles).

with significantly more chemostatic (closer to 0) responses in lake influenced Oksrukuyik than in the Kuparuk (Tukey's test, $p < 0.05$). For TDN, we found no significant differences between watershed *C-Q* slopes, but there was a strong effect of year on β indicating interannual variability in TDN *C-Q* response (ANOVA; $F_{4, 58} = 3.433$, $p = 0.01$). Across all years, CV_C/CV_Q ratios were generally less than 1 (Figures 4d–4e).

Across our watersheds, we found no statistical relationship between paired DOC and NO_3^- or TDN *C-Q* β at the event-scale based on simple linear regressions ($p > 0.05$ for all models). However, we did observe general patterns in paired *C-Q* behavior, where storm events fell predictably within a quadrant on a biplot between DOC

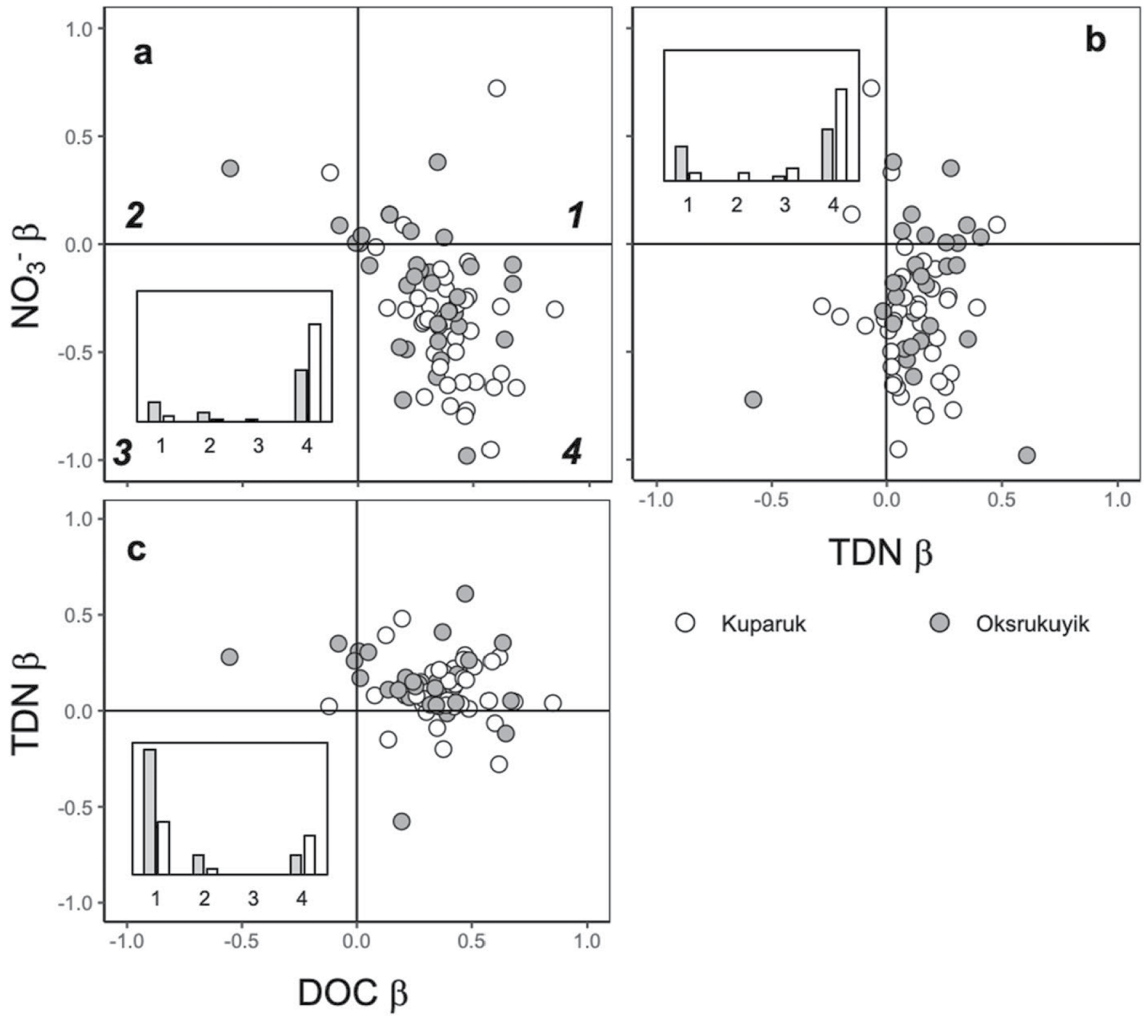

Figure 5. Biplots of event-scale *C-Q* β of (a) NO_3^- versus dissolved organic carbon (DOC), (b) NO_3^- versus total dissolved nitrogen (TDN), and (c) TDN versus DOC for the Kuparuk River (white circles) and Oksrukuyik Creek (gray circles) from 2017 to 2021. Quadrants (1–4) represent the following responses: (1) Convergent *C-Q* enrichment of C and N, (2) Divergent *C-Q* N enrichment, C dilution, (3) Convergent *C-Q* dilution of C and N, and (4) Divergent *C-Q* C enrichment, N dilution. Histograms of quadrant counts for each biplot are inseted into each panel.

(*x-axis*) and nitrogen species (NO_3^- and TDN, *y-axis*) (Figure 5). In both the Kuparuk and Oksrukuyik watersheds, DOC and NO_3^- *C-Q* responses were primarily divergent, falling in quadrant 4 indicating DOC enrichment while NO_3^- diluted. In contrast, the DOC and TDN *C-Q* responses were convergently enriched, falling in quadrant 1 (Figure 5).

Our DOC k_C values were consistently negative, indicating a decline in concentration during the falling limb of the hydrograph (Figure 6a). We observed no significant difference in DOC k_C between watersheds (ANOVA, $p > 0.05$), but we found a significant effect of year on DOC k_C, likely the result of interannual variability in flow (ANOVA, $p = 0.001$, Figure 2). In general, NO_3^- k_C values were positive, indicating that instream concentrations increased as discharge returned to pre-event flows (Figure 6b). We found no significant effect of the watershed on NO_3^- k_C (ANOVA, $p > 0.05$), but there was significant variability in means across sampling years for both metrics ($p = p < 0.05$). Generally, we observed slower, "lagged" values of NO_3^- k_C *relative* to DOC k_C (Figure 6b). Conversely, TDN recession constants followed a similar trend to DOC (Figure 6c). We did not observe any significant seasonal trends for DOC, NO_3^-, or TDN k_C (Figure S7 in Supporting Information S1). We then compared the concentration recession constants for both watersheds to explore post-event recovery of DOC and N species, as shown in Figure 7. We found significant relationships between DOC and NO_3^- concentration recovery (as k_C) (*Kuparuk:* $R^2 = 0.19$, $p < 0.001$; *Oksrukuyik:* $R^2 = 0.24$, $p < 0.01$), with a divergence in C versus

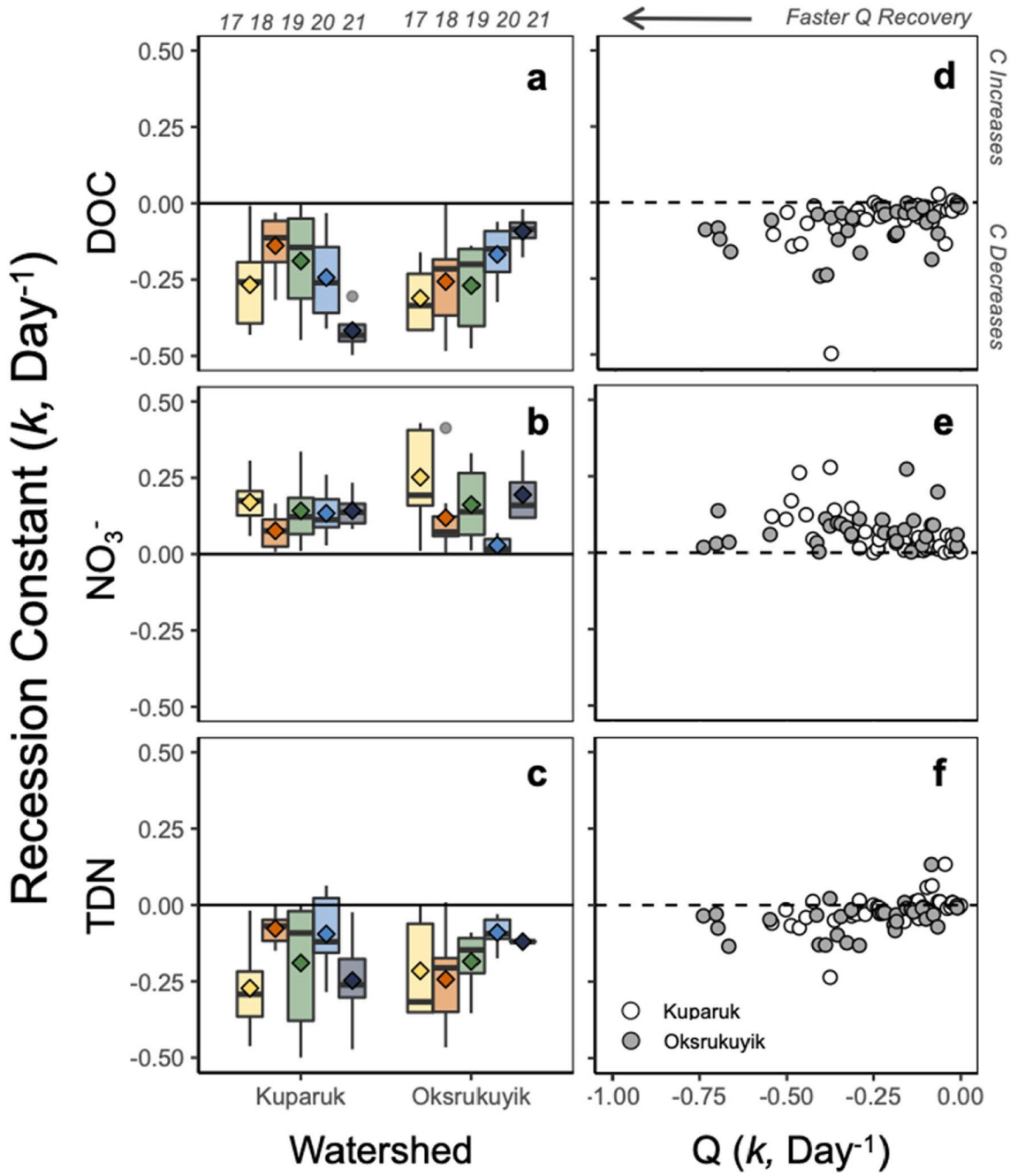

Figure 6. Boxplots of recession constants for concentration (k_C) for (a) dissolved organic carbon (DOC), (b) Nitrate (NO_3^-), and (c) total dissolved nitrogen (TDN) for the Kuparuk and Oksrukuyik watersheds from 2017 (yellow), 2018 (orange), 2019 (green), 2020 (blue), and 2021 (gray). Annual mean and median k are reported as a point and horizontal bar, respectively. Note the horizontal reference line at $y = 0$, where $k > 0$ indicates that the solute increases during the event recession and $k < 0$ suggests solute decreases after the event recession. We also include a comparison of the discharge recession (k_Q) versus k_C for (d) DOC, (e) NO_3^-, and (f) TDN for the Kuparuk (white circles) and Oksrukuyik (gray circles).

N concentration response to storm recession (Figures 7a and 7c). Conversely, our k_C values for DOC versus TDN were nearly equivalent where both constituents decreased after peak flow, and this relationship was strongly linear (*Kuparuk:* $R^2 = 0.78$, $p < 0.001$; *Oksrukuyik:* $R^2 = 0.68$, $p < 0.01$) (Figures 7b and 7d).

Across both watersheds, the organic N fraction (DON) consistently constitutes a high proportion of TDN relative to DIN. Across all years, the mean (± standard error) TDN concentrations from grab samples were 0.72 ± 0.034 mg/L for the Kuparuk and 0.70 ± 0.069 mg/L for Oksrukuyik. In the Kuparuk, ammonium (NH_4+)

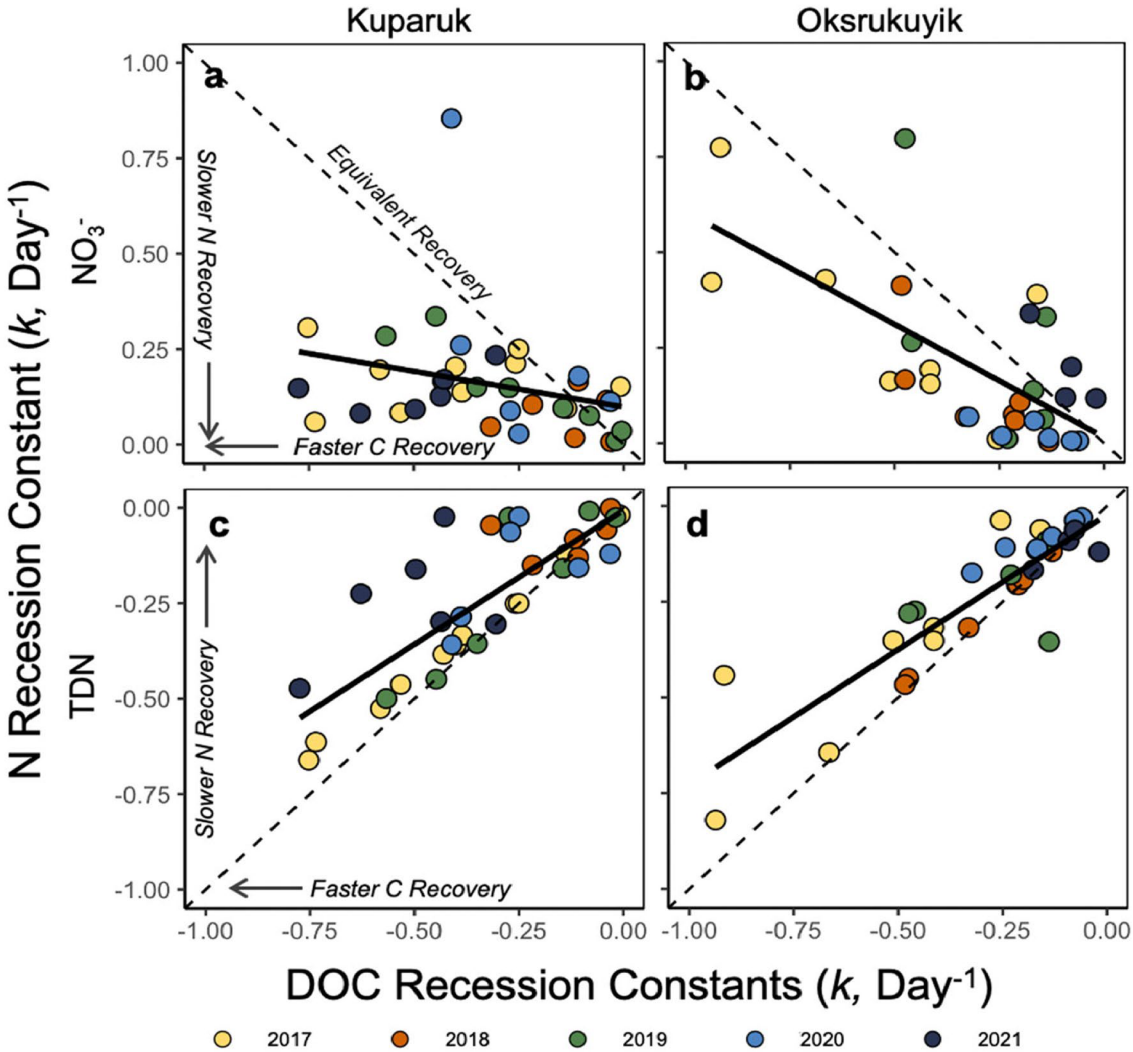

Figure 7. Biplots of event-scale *C-Q* recession constants for concentration (k_C) of (a, b). NO_3^- versus dissolved organic carbon (DOC) and (c, d) total dissolved nitrogen versus DOC for the Kuparuk and Oksrukuyik watersheds from 2017 (yellow), 2018 (orange), 2019 (green), 2020 (blue), and 2021 (gray).

concentrations are low (0.022 ± 0.016 mg/L), such that NO_3 (0.15 ± 0.03 mg/L) represents the larger fraction of DIN. From these values, DIN is approximately 25% of the TDN pool. Similarly, for Oksrukuyik, NH_4+ (0.021 ± 0.010 mg/L) and NO_3 (0.084 ± 0.018 mg/L) constitute about 15% of TDN, with DON representing the remaining 85% by subtraction. Considering the high organic proportion, the relationship between DOC and TDN concentration recovery is likely indicative of the dominance of organic N fractions co-mobilized with organic matter (Figure S8 in Supporting Information S1).

5. Discussion

5.1. Event-Scale C-Q Metrics Indicate Divergent Behavior Between DOC and NO_3^-

The expectation that storms represent a major disturbance to C and N transport and processing has become well-established in ecosystem theory, including the "flood pulse" (Junk et al., 1989), "pulse-shunt" (Raymond et al., 2016), "variable source area" and "nutrient source area sequencing" (Bernier, 1985; Betson, 1964; Dunne & Black, 1970; McGlynn & McDonnell, 2003), and the "river network saturation" concepts (Wollheim et al., 2018). Together, these frameworks predict that storms mobilize available material from terrestrial to aquatic ecosystems through subsurface and surface flow paths (Chorover et al., 2017). As mobilization increases during high flows, streams begin to transport more material than they can process, changing the river from a net transformer to a net

transporter of material downstream (Casas-Ruiz et al., 2020; Fazekas et al., 2021). Such hydro-biogeochemical concepts have revealed the dynamical nature of river responses that can be captured in an integrated watershed response such as *C-Q* behavior across temperate and high-latitude regions (Blaen et al., 2017; Fazekas et al., 2020; Khamis et al., 2021; Musolff et al., 2017, 2018; Rose et al., 2018; Shogren et al., 2021; Vaughan et al., 2017; Webster et al., 2021; Zimmer et al., 2019).

Here, we expanded upon previous work that demonstrated that landscape attributes, such as slope and the presence of stream-lake chains, influence the emergent watershed *C-Q* responses for carbon and nutrients (Shogren et al., 2021). In the present study, we found that DOC and NO_3^- were consistently exported divergently from our two study watersheds, indicative of a substantive stoichiometric shift in DOC:NO_3^- at the event-scale. In both the Kuparuk and Oksrukuyik Creek watersheds, concentrations of DOC were predictably elevated while NO_3^- concentrations decreased with increasing flows. Overall, these findings are intuitive for tundra streams on the North Slope of Alaska, which are typically N-limited (Khosh et al., 2017), where mobilization is limited by a small source pool of DIN (Harms & Jones, 2012; Townsend-Small et al., 2011). The results are also consistent with the assumption that terrestrial organic matter pools in the Arctic are in ample supply, but must be hydrologically activated to mobilize into the river network (Khamis et al., 2021; Shogren et al., 2021). The temporary elevation of DOC relative to NO_3^- concentrations during storm events observed in both watersheds suggests that storm events represent not only a hydrologic disturbance but also a consistent driver of landscape stoichiometric imbalance as the river network transitions between reactor-to pipe-like conditions (Wollheim et al., 2018). Surprisingly, seasonal changes did not manifest in seasonal trends in *C-Q* responses for paired DOC and NO_3^- (Figures S6 and S7 in Supporting Information S1). For example, we expected that seasonal deepening of the active layer would manifest in temporal changes in DOC:NO_3^- *C-Q* responses resulting from shifts in N-demand and evolving subsurface flowpaths (Evans & Ge, 2017). However, the consistent values of $CV_C/CV_Q < 1$ indicate that the co-transport of C and N is more strongly controlled by variability in hydrology than the ability of biogeochemical processes to exert control over the export of these solutes (Wymore et al., 2021). Our observations suggest that network topology and hydrologic context play a significant role in driving C and N co-exports and their resulting proportions, which are more influential than active layer dynamics alone in our study watersheds (Connolly et al., 2018; Harms et al., 2016; Khosh et al., 2017; Tank et al., 2020; Vonk et al., 2019).

Another unique finding in this study is the prevalence of TDN enrichment ($\beta > 0$) in our two study watersheds, representing a strong stoichiometric coupling between the organic N fraction and DOC which are co-mobilized during storms. DON constitutes a large fraction of the TDN transported in Arctic rivers (Kaiser et al., 2017) and is related to the bioavailability of DOM (Wickland et al., 2018). River exports of DON serve as important resources for Arctic ecosystems, including larger freshwater lakes (Levine & Whalen, 2001; MacIntyre et al., 2006), coastal environments (Amon & Meon, 2004; McClelland et al., 2014; Tank et al., 2012), and ultimately the Arctic Ocean (Dittmar, 2004; Dittmar et al., 2001; Letscher et al., 2013; Paulsen et al., 2018). Our TDN results suggest that a large DON fraction may leach from Arctic ecosystems during storm events despite strong terrestrial and aquatic biotic demand for inorganic N (Liu et al., 2018; Neff et al., 2003). Furthermore, hydrologically mediated export may help DON effectively bypass microbial processing in permafrost soils and within stream processes. Effectively, DON represents both a source and sink of aquatic N (Neff et al., 2003), depending on the lability of the parent material and processing time. DON can be a downstream source of inorganic N when processing by microbes or photodegradation releases DIN (Bowen, 2021), or it can be considered a sink when it is mobilized downstream and transported toward the Arctic Ocean (Tank et al., 2012). As Arctic storms become more frequent and intense, understanding the contributions of DON to the redistribution of N resources across the landscape will be an important constraint on aquatic and terrestrial productivity (Francis et al., 2023).

5.2. Post-Event Recovery Indicates Different Recovery of DOC:NO_3^-

Our findings highlight that storm events are likely to elevate instream DOC:NO_3^- ratios for multiple days in low-gradient tundra streams. In other words, a storm event may exacerbate N-limitation as material is redistributed across the landscape, where elevated C:DIN is sustained. Our results for DOC:NO_3^-, including the lack of seasonal trends, can be explained by several non-exclusive scenarios that account for different dominant processes controlling DOC versus NO_3^- exports as thaw depth thickens and flow paths evolve. At the start of active river flow in the Arctic, event runoff travels via surface runoff or through shallow, organic-rich soil layers (Finlay et al., 2006; Paquette et al., 2018). As an event recedes, watersheds may simply experience a reduction in DOC

concentration as these hydrologically connected source areas become rapidly disconnected, slowing the transport capacity of carbon (Burns et al., 2016; Goodwell et al., 2018). As thaw depth progresses toward the seasonal maxima, the rapid return to pre-event conditions likely reflects the steeper vertical gradient of soil organic matter content relative to depth (Connolly et al., 2018), thus changing hydrologic flow paths that contribute DOC to the stream channel (Ågren et al., 2014; Voytek et al., 2016). For example, the active layer may become saturated during stormflow, such that translatory flow quickly flushes older, DOC-concentrated water into the stream channel from riparian zones (Boyer et al., 1997; Weiler & McDonnell, 2006), and supply slows after the storm event. Alternatively, saturated excess overland flow might result in event-water that is routed preferentially through the shallow organic horizons, resulting in a rapid conveyance of solutes downslope from transmissive soils (Boyer et al., 1997; Neilson et al., 2018). As the storm recedes, water flow-paths may transition back to deeper C-poor mineral horizons (Krogh et al., 2017; MacLean et al., 1999), resulting in a rapid decline of observed instream DOC concentrations. While we cannot accurately parse the mechanisms contributing to material and water flow with this study, the mechanisms of flow and solute generation remain a critical data gap in high-latitude science (Vonk et al., 2019; Voytek et al., 2016).

Meanwhile, the lagged behavior of recovery in NO_3^- may represent a combined effect of both hydrologic and biogeochemical controls on transporting and producing DIN into the stream network. During the storm, N dilution is likely the consequence of the increased flow and limited terrestrial N availability (Ensign & Doyle, 2006). After a storm disturbance, a slow NO_3^- recovery may simply reflect decreasing hydrologic dilution of DIN: as discharge decreases low concentrations slowly rise to baseline. Alternatively, the mismatch in DOC:NO_3^- recovery rates may also reflect variability in post-disturbance biotic processes, such as altered terrestrial or instream biotic demand of DIN. The stream channel may have reduced streambed assimilatory capacity after peak flows, when benthic biofilms are scoured, and light availability is lessened (McNamara et al., 2008), thus allowing NO_3^- to recover more quickly relative to DOC. Flood pulses may also enhance land-water connectivity, increasing biological N uptake by microbes and plants in the riparian zone and thereby limiting N export into the stream channel (Harms & Ludwig, 2016). The ability of stream riparian zones to rapidly take up inorganic forms of N has been noted in permafrost soils (Pastor et al., 2020). While our study did not directly measure hillslope riparian production or reach-scale uptake of NO_3^- during or after peak flows (Covino et al., 2021; Harms et al., 2019), our results indicate that the combined effect of elevated DOC, reduced NO_3^- availability, and limited instream uptake capacity may contribute to a delay in biogeochemical recovery after a strong event disturbance.

5.3. Implications of C-Q Metrics for Arctic Watersheds

Our sampling efforts further define Arctic storms as major biogeochemical disruptors, with the capacity to differentially export and redistribute C and N that are hydrologically mobilized from land to water. In our study watersheds, storm events may elevate DOC:NO_3 ratios that are slow to recover from hydrologic disturbance while increasing exports of TDN. Additionally, the application of a chemograph recession constant k_C provides additional evidence for a prolonged instream NO_3^- recovery response relative to available DOC stores. Overall, our findings highlight that storm events play an important role in the co-exports of C and N in intermediate-scale (<100 km^2) Arctic headwaters, which represent a significant source of uncertainty in high-latitude biogeochemical budgets (Starr et al., 2023). Notably, patterns of non-changing riverine fluxes of DOC concurrent with declining fluxes of NO_3^- have emerged at larger watershed scales (>10,000 km^2) (Tank et al., 2023), while increasing exports of DON (a large portion of TDN) have significant implications for productivity of the Arctic Ocean (Tank et al., 2012). While changes in fluxes observed at the large catchment scale represent many competing mechanisms that drive the directional shifts in N concentrations, these changes likely start far upstream. That is, if fluxes of N relative to C are changing significantly in large Arctic rivers, this is the result of the combination of systemic changes experienced by the upstream headwaters, where signals are maintained as water flows toward the Arctic Ocean. Therefore, capturing the C and N transport and transformation from headwater-scale Arctic landscapes under different climactic and ecological conditions must remain a priority for predicting and observing changes to high latitude regions (Shogren et al., 2020; Virkkala et al., 2019; Vonk et al., 2023).

Despite rapid changes to high-latitude ecosystems evident in changing river chemistry, research efforts in Arctic rivers have lagged behind those in temperate regions (Laudon et al., 2017). The spring snowmelt and mid-season storm events are predicted to become more intense (Blaskey et al., 2023; Dou et al., 2022), resulting in seasonal and interannual changes in the magnitude of C and N transported from Arctic headwaters. In recent years, optical

sensors have provided a useful tool to help quantify additional solutes of interest (Burns et al., 2019; Crawford et al., 2015; Pellerin et al., 2016; Rode et al., 2016). We encourage exploration and expansion of high-frequency monitoring in an effort to expand our understanding of biogeochemical conditions in a changing Arctic, but wish to provide a word of caution. While it can be tempting to rely on the sensor-derived parameters or established calibration relationships, concentration estimates from sensors must be bolstered with effort to validate these relationships across space and over time. We emphasize the importance of generating unique solute-, watershed-, and year-specific calibration models (Figures S1–S5 in Supporting Information S1) to adequately predict time-series of concentrations or the user risks significant over-interpretation of the high-frequency records. Despite these modest challenges, the application of high-frequency water quality sensors in Arctic regions still provides an exciting solution for capturing the varying influence of landscape on hydrochemical attributes that drive longitudinal and lateral solute fluxes (Shogren et al., 2021; Zarnetske et al., 2020a , 2020b, 2020c). The lateral flux of C and N to Arctic river networks thus remains a significant source of uncertainty in constraining biogeochemical budgets in high-latitude ecosystems as the Arctic hydrologic cycle shifts toward more intense precipitation (McCrystall et al., 2021).

Conflict of Interest

The authors declare no conflicts of interest relevant to this study.

Data Availability Statement

The *C-Q* metrics and recession constants are available as a supplemental data file (Data Set S1). A subset of the high-frequency data included in this study are publically available through the Environmental Data Initiative (EDI) (2017–2019) (Zarnetske et al., 2020a, 2020b). Additional data that are included in this study (e.g., 2020–2021 high frequency data) have been uploaded to the ADC as required by NSF-OPP's data sharing policies (Shogren et al., 2023a, 2023b). The ADC is a permanent repository that follows Collective benefit, Authority to control, Responsibility, and Ethics (CARE) principles, which is complimentary to Findable, Accessible, Interoperable, and Reproducible (FAIR) data management principles aligned with AGU open data policies.

Acknowledgments

Data and facilities were provided by the Arctic LTER at Toolik Field Station (NSF-DBI-1637459). The authors gratefully acknowledge the Arctic LTER, the Toolik Environmental Data Center (EDC), Toolik Field Station staff, and CH2M HILL Polar Services for assistance in support of this work, particularly during the challenging 2020 field season. DEMs were provided by the Polar Geospatial Center under NSF-OPP awards 1043681, 1559691, and 1542736. The authors would also like to acknowledge their funding support: AJS (NSF-OPP-1916567); JPZ, AG, CS (NSF-EAR-1846855, NSF-OPP-1916567); BWA, JN, JO (NSF-OPP-1916565); WBB, AR (NSF-OPP-1916576, NSF DBI-1637459). We wish to acknowledge that our field sites are located on the homelands and hunting grounds of the Nunamiut, and the occasional hunting grounds and routes of the Gwich'in, Koyukuk, and Iñupiaq peoples.

References

Abbott, B. W., Jones, J. B., Godsey, S. E., Larouche, J. R., & Bowden, W. B. (2015). Patterns and persistence of hydrologic carbon and nutrient export from collapsing upland permafrost. *Biogeosciences*, *12*(12), 3725–3740. https://doi.org/10.5194/bg-12-3725-2015

Abbott, B. W., Rocha, A. V., Shogren, A., Zarnetske, J. P., Iannucci, F., Bowden, W. B., et al. (2021). Tundra wildfire triggers sustained lateral nutrient loss in Alaskan Arctic. *Global Change Biology*, *27*(7), 1408–1430. https://doi.org/10.1111/gcb.15507

Ågren, A. M., Buffam, I., Cooper, D. M., Tiwari, T., Evans, C. D., & Laudon, H. (2014). Can the heterogeneity in stream dissolved organic carbon be explained by contributing landscape elements? *Biogeosciences*, *11*(4), 1199–1213. https://doi.org/10.5194/bg-11-1199-2014

Amon, R. M. W., & Meon, B. (2004). The biogeochemistry of dissolved organic matter and nutrients in two large Arctic estuaries and potential implications for our understanding of the Arctic Ocean system. *Marine Chemistry*, *92*, 311–330. https://doi.org/10.1016/j.marchem.2004.06.034

Beel, C., Heslop, J., Orwin, J., Pope, M., Schevers, A., Hung, J., et al. (2020). Emerging dominance of summer rainfall in driving High Arctic terrestrial-aquatic connectivity (Preprint). In Review. https://doi.org/10.21203/rs.3.rs-76410/v1

Bernier, P. Y. (1985). Variable source areas and storm-flow generation: An update of the concept and a simulation effort. *Journal of Hydrology*, *79*(3), 195–213. https://doi.org/10.1016/0022-1694(85)90055-1

Betson, R. P. (1964). What is watershed runoff? *Journal of Geophysical Research*, *69*(8), 1541–1552. https://doi.org/10.1029/JZ069i008p01541

Bintanja, R., & Andry, O. (2017). Towards a rain-dominated Arctic. *Nature Climate Change*, *7*(4), 263–267. https://doi.org/10.1038/nclimate3240

Blaen, P. J., Khamis, K., Lloyd, C., Comer-Warner, S., Ciocca, F., Thomas, R. M., et al. (2017). High-frequency monitoring of catchment nutrient exports reveals highly variable storm event responses and dynamic source zone activation. *Journal of Geophysical Research: Biogeosciences*, *122*(9), 2265–2281. https://doi.org/10.1002/2017JG003904

Blaskey, D., Koch, J. C., Gooseff, M. N., Newman, A. J., Cheng, Y., O'Donnell, J. A., & Musselman, K. N. (2023). Increasing Alaskan river discharge during the cold season is driven by recent warming. *Environmental Research Letters*, *18*(2), 024042. https://doi.org/10.1088/1748-9326/acb661

Bond, N. (2019). Package "hydrostats.". *R Documentation*, *1–29*.

Bowen, J. (2021). Impact of dissolved organic matter photodegradation on carbon and nitrogen cycling in freshwaters. [Thesis]. https://doi.org/10.7302/3033

Boyer, E. W., Hornberger, G. M., Bencala, K. E., & McKnight, D. M. (1997). Response characteristics of DOC flushing in an alpine catchment. *Hydrological Processes*, *11*(12), 1635–1647. https://doi.org/10.1002/(SICI)1099-1085(19971015)11:12<1635::AID-HYP494>3.0.CO;2-H

Bring, A., Fedorova, I., Dibike, Y., Hinzman, L., Mård, J., Mernild, S. H., et al. (2016). Arctic terrestrial hydrology: A synthesis of processes, regional effects, and research challenges. *Journal of Geophysical Research: Biogeosciences*, *121*(3), 621–649. https://doi.org/10.1002/2015JG003131

Brutsaert, W., & Nieber, J. L. (1977). Regionalized drought flow hydrographs from a mature glaciated plateau. *Water Resources Research*, *13*(3), 637–643. https://doi.org/10.1029/WR013i003p00637

Burgin, A. J., & Hamilton, S. K. (2007). Have we overemphasized the role of denitrification in aquatic ecosystems? A review of nitrate removal pathways. *Frontiers in Ecology and the Environment*, *5*(2), 89–96. https://doi.org/10.1890/1540-9295(2007)5[89:HWOTRO]2.0.CO;2

Burns, M. A., Barnard, H. R., Gabor, R. S., McKnight, D. M., & Brooks, P. D. (2016). Dissolved organic matter transport reflects hillslope to stream connectivity during snowmelt in a montane catchment. *Water Resources Research*, *52*(6), 4905–4923. https://doi.org/10.1002/2015WR017878

Burns, D. A., Pellerin, B. A., Miller, M. P., Capel, P. D., Tesoriero, A. J., & Duncan, J. M. (2019). Monitoring the riverine pulse: Applying high-frequency nitrate data to advance integrative understanding of biogeochemical and hydrological processes. *Wiley Interdisciplinary Reviews: Water*, e1348. https://doi.org/10.1002/wat2.1348

Casas-Ruiz, J. P., Spencer, R. G. M., Guillemette, F., von Schiller, D., Obrador, B., Podgorski, D. C., et al. (2020). Delineating the continuum of dissolved organic matter in temperate river networks. *Global Biogeochemical Cycles*, *34*(8), e2019GB006495. https://doi.org/10.1029/2019GB006495

Chorover, J., Derry, L. A., & McDowell, W. H. (2017). Concentration-discharge relations in the critical zone: Implications for resolving critical zone structure, function, and evolution. *Water Resources Research*, *53*(11), 8654–8659. https://doi.org/10.1002/2017WR021111

Connolly, C. T., Khosh, M. S., Burkart, G. A., Douglas, T. A., Holmes, R. M., Jacobson, A. D., et al. (2018). Watershed slope as a predictor of fluvial dissolved organic matter and nitrate concentrations across geographical space and catchment size in the Arctic. *Environmental Research Letters*, *13*(10). 104015. https://doi.org/10.1088/1748-9326/aae35d

Conroy, N. A., Dann, J. B., Newman, B. D., Heikoop, J. M., Arendt, C., Busey, B., et al. (2022). Chemostatic concentration–discharge behaviour observed in a headwater catchment underlain with discontinuous permafrost. *Hydrological Processes*, *36*(5), e14591. https://doi.org/10.1002/hyp.14591

Covino, T. P., Wlostowski, A. N., Gooseff, M. N., Wollheim, W. M., & Bowden, W. B. (2021). The seasonality of in-stream nutrient concentrations and uptake in arctic headwater streams in the northern foothills of Alaska's Brooks range. *Journal of Geophysical Research: Biogeosciences*, *126*(4), e2020JG005949. https://doi.org/10.1029/2020JG005949

Crawford, J. T., Loken, L. C., Casson, N. J., Smith, C., Stone, A. G., & Winslow, L. A. (2015). High-speed limnology: Using advanced sensors to investigate spatial variability in biogeochemistry and hydrology. *Environmental Science & Technology*, *49*(1), 442–450. https://doi.org/10.1021/es504773x

Dery, S. J., Stieglitz, M., Rennermalm, A. K., & Wood, E. F. (2005). The water budget of the Kuparuk River basin, Alaska. *Journal of Hydrometeorology*, *6*(5), 633–655. https://doi.org/10.1175/JHM434.1

Dittmar, T. (2004). Evidence for terrigenous dissolved organic nitrogen in the Arctic deep sea. *Limnology & Oceanography*, *49*(1), 148–156. https://doi.org/10.4319/lo.2004.49.1.0148

Dittmar, T., Fitznar, H. P., & Kattner, G. (2001). Origin and biogeochemical cycling of organic nitrogen in the eastern Arctic Ocean as evident from D- and L-amino acids. *Geochimica et Cosmochimica Acta*, *65*(22), 4103–4114. https://doi.org/10.1016/S0016-7037(01)00688-3

Dou, T. F., Pan, S. F., Bintanja, R., & Xiao, C. D. (2022). More frequent, intense, and extensive rainfall events in a strongly warming Arctic. *Earth's Future*, *10*(10), e2021EF002378. https://doi.org/10.1029/2021EF002378

Drake, C. W., Jones, C. S., Schilling, K. E., Amado, A. A., & Weber, L. J. (2018). Estimating nitrate-nitrogen retention in a large constructed wetland using high-frequency, continuous monitoring and hydrologic modeling. *Ecological Engineering*, *117*, 69–83. https://doi.org/10.1016/j.ecoleng.2018.03.014

Dunne, T., & Black, R. D. (1970). Partial area contributions to storm runoff in a small New England watershed. *Water Resources Research*, *6*(5), 1296–1311. https://doi.org/10.1029/WR006i005p01296

Ebel, B. A., Koch, J. C., & Walvoord, M. A. (2019). Soil physical, hydraulic, and thermal properties in interior Alaska, USA: Implications for hydrologic response to thawing permafrost conditions. *Water Resources Research*, *55*(5), 4427–4447. https://doi.org/10.1029/2018WR023673

Edwards, A. C., Hooda, P. S., & Cook, Y. (2001). Determination of nitrate in water containing dissolved organic carbon by ultraviolet spectroscopy. *International Journal of Environmental Analytical Chemistry*, *80*(1), 49–59. https://doi.org/10.1080/03067310108044385

Ensign, S. H., & Doyle, M. W. (2006). Nutrient spiraling in streams and river networks. *Journal of Geophysical Research*, *111*(G4). https://doi.org/10.1029/2005JG000114

Ernakovich, J. G., Hopping, K. A., Berdanier, A. B., Simpson, R. T., Kachergis, E. J., Steltzer, H., & Wallenstein, M. D. (2014). Predicted responses of arctic and alpine ecosystems to altered seasonality under climate change. *Global Change Biology*, *20*(10), 3256–3269. https://doi.org/10.1111/gcb.12568

Etheridge, J. R., Birgand, F., Osborne, J. A., Osburn, C. L., Burchell, M. R., & Irving, J. (2014). Using in situ ultraviolet-visual spectroscopy to measure nitrogen, carbon, phosphorus, and suspended solids concentrations at a high frequency in a brackish tidal marsh. *Limnology and Oceanography: Methods*, *12*(1), 10–22. https://doi.org/10.4319/lom.2014.12.10

Evans, S. G., & Ge, S. (2017). Contrasting hydrogeologic responses to warming in permafrost and seasonally frozen ground hillslopes. *Geophysical Research Letters*. https://doi.org/10.1002/2016GL072009

Fan, Y., Clark, M., Lawrence, D. M., Swenson, S., Band, L. E., Brantley, S. L., et al. (2019). Hillslope hydrology in global change research and Earth system modeling. *Water Resources Research*, *55*(2), 1737–1772. https://doi.org/10.1029/2018WR023903

Fazekas, H. M., McDowell, W. H., Shanley, J. B., & Wymore, A. S. (2021). Climate variability drives watersheds along a transporter-transformer continuum. *Geophysical Research Letters*, *48*(21), e2021GL094050. https://doi.org/10.1029/2021GL094050

Fazekas, H. M., Wymore, A. S., & McDowell, W. H. (2020). Dissolved organic carbon and nitrate concentration-discharge behavior across scales: Land use, excursions, and misclassification. *Water Resources Research*, *56*(8), e2019WR027028. https://doi.org/10.1029/2019WR027028

Finlay, J., Neff, J., Zimov, S., Davydova, A., & Davydov, S. (2006). Snowmelt dominance of dissolved organic carbon in high-latitude watersheds: Implications for characterization and flux of river DOC. *Geophysical Research Letters*, *33*(10), L10401. https://doi.org/10.1029/2006GL025754

Francis, A., Ganeshram, R. S., Tuerena, R. E., Spencer, R. G. M., Holmes, R. M., Rogers, J. A., & Mahaffey, C. (2023). Permafrost degradation and nitrogen cycling in Arctic rivers: Insights from stable nitrogen isotope studies. *Biogeosciences*, *20*(2), 365–382. https://doi.org/10.5194/bg-20-365-2023

Frei, R. J., Abbott, B. W., Dupas, R., Gu, S., Gruau, G., Thomas, Z., et al. (2020). Predicting nutrient incontinence in the anthropocene at watershed scales. *Frontiers in Environmental Science*, *7*. https://www.frontiersin.org/article/10.3389/fenvs.2019.00200

Frey, K. E., & McClelland, J. W. (2009). Impacts of permafrost degradation on arctic river biogeochemistry. *Hydrological Processes*, *23*(1), 169–182. https://doi.org/10.1002/hyp.7196

Godsey, S. E., Hartmann, J., & Kirchner, J. W. (2019). Catchment chemostasis revisited: Water quality responds differently to variations in weather and climate. *Hydrological Processes*, *33*(24), 3056–3069. https://doi.org/10.1002/hyp.13554

Godsey, S. E., Kirchner, J. W., & Clow, D. W. (2009). Concentration–discharge relationships reflect chemostatic characteristics of US catchments. *Hydrological Processes*, *23*(13), 1844–1864. https://doi.org/10.1002/hyp.7315

Goodwell, A. E., Kumar, P., Fellows, A. W., & Flerchinger, G. N. (2018). Dynamic process connectivity explains ecohydrologic responses to rainfall pulses and drought. *Proceedings of the National Academy of Sciences of the United States of America*, *115*(37), E8604–E8613. https://doi.org/10.1073/pnas.1800236115

Gorski, G., & Zimmer, M. A. (2021). Hydrologic regimes drive nitrate export behavior in human-impacted watersheds. *Hydrology and Earth System Sciences*, *25*(3), 1333–1345. https://doi.org/10.5194/hess-25-1333-2021

Griffith, D. M., & Anderson, T. M. (2019). The 'plantspec' r package: A tool for spectral analysis of plant stoichiometry. *Methods in Ecology and Evolution*, *10*(5), 673–679. https://doi.org/10.1111/2041-210X.13143

Gunderson, L. H. (2000). Ecological resilience—In theory and application. *Annual Review of Ecology and Systematics*, *31*, 425–439.

Hamilton, T. D. (2003). Surficial geology of the Dalton Highway (Itkillik-Sagavanirktok rivers) area, southern Arctic foothills. https://doi.org/10.14509/7191

Harms, T. K., Cook, C. L., Wlostowski, A. N., Gooseff, M. N., & Godsey, S. E. (2019). Spiraling down hillslopes: Nutrient uptake from water tracks in a warming arctic. *Ecosystems*, *22*, 1546–1560. https://doi.org/10.1007/s10021-019-00355-z

Harms, T. K., Edmonds, J. W., Genet, H., Creed, I. F., Aldred, D., Balser, A., & Jones, J. B. (2016). Catchment influence on nitrate and dissolved organic matter in Alaskan streams across a latitudinal gradient. *Journal of Geophysical Research: Biogeosciences*, *121*(2), 350–369. https://doi.org/10.1002/2015JG003201

Harms, T. K., & Jones, J. (2012). Thaw depth determines reaction and transport of inorganic nitrogen in valley bottom permafrost soils: Nitrogen cycling in permafrost soils. *Global Change Biology*, *18*, 2958–2968. https://doi.org/10.1111/j.1365-2486.2012.02731.x

Harms, T. K., & Ludwig, S. M. (2016). Retention and removal of nitrogen and phosphorus in saturated soils of arctic hillslopes. *Biogeochemistry*, *127*(2–3), 291–304. https://doi.org/10.1007/s10533-016-0181-0

Helton, A. M., Ardón, M., & Bernhardt, E. S. (2015). Thermodynamic constraints on the utility of ecological stoichiometry for explaining global biogeochemical patterns. *Ecology Letters*, *18*(10), 1049–1056. https://doi.org/10.1111/ele.12487

J. E. Hobbie, & G. W. Kling (Eds.), (2014). *Alaska's changing Arctic*. Oxford University Press. https://doi.org/10.1093/acprof:osobl/9780199860401.001.0001

Holling, C. S. (1973). Resilience and stability of ecological systems. *Annual Review of Ecology and Systematics*, *4*(1), 1–23. https://doi.org/10.1146/annurev.es.04.110173.000245

Inamdar, S. P., O'Leary, N., Mitchell, M. J., & Riley, J. T. (2006). The impact of storm events on solute exports from a glaciated forested watershed in western New York, USA. *Hydrological Processes*, *20*(16), 3423–3439. https://doi.org/10.1002/hyp.6141

Junk, W. J., Bayley, P. B., & Sparks, R. E. (1989). The flood pulse concept in river-floodplain systems. *Canadian Special Publication of Fisheries and Aquatic Sciences*, *106*(1), 110–127. https://doi.org/10.1371/journal.pone.0028909

Kaiser, K., Canedo-Oropeza, M., McMahon, R., & Amon, R. M. W. (2017). Origins and transformations of dissolved organic matter in large Arctic rivers. *Scientific Reports*, *7*(1). 13064. https://doi.org/10.1038/s41598-017-12729-1

Khamis, K., Blaen, P. J., Comer-Warner, S., Hannah, D. M., MacKenzie, A. R., & Krause, S. (2021). High-frequency monitoring reveals multiple frequencies of nitrogen and carbon mass balance dynamics in a headwater stream. *Frontiers in Water*, *3*. https://doi.org/10.3389/frwa.2021.668924

Khosh, M. S., McClelland, J. W., Jacobson, A. D., Douglas, T. A., Barker, A. J., & Lehn, G. O. (2017). Seasonality of dissolved nitrogen from spring melt to fall freezeup in Alaskan Arctic tundra and mountain streams. *Journal of Geophysical Research: Biogeosciences*, *122*(7), 1718–1737. https://doi.org/10.1002/2016JG003377

Kicklighter, D. W., Hayes, D. J., McClelland, J. W., Peterson, B. J., McGuire, A. D., & Melillo, J. M. (2013). Insights and issues with simulating terrestrial DOC loading of Arctic river networks. *Ecological Applications*, *23*(8), 1817–1836. https://doi.org/10.1890/11-1050.1

Kincaid, D. W., Seybold, E. C., Adair, E. C., Bowden, W. B., Perdrial, J. N., Vaughan, M. C. H., & Schroth, A. W. (2020). Land use and season influence event-scale nitrate and soluble reactive phosphorus exports and export stoichiometry from headwater catchments. *Water Resources Research*, *56*(10), e2020WR027361. https://doi.org/10.1029/2020WR027361

Knapp, J. L. A., Freyberg, J., Studer, B., Kiewiet, L., & Kirchner, J. W. (2020). Concentration–discharge relationships vary among hydrological events, reflecting differences in event characteristics. *Hydrology and Earth System Sciences*, *24*(5), 2561–2576. https://doi.org/10.5194/hess-24-2561-2020

Kokelj, S. V., & Jorgenson, M. T. (2013). Advances in thermokarst research. *Permafrost and Periglacial Processes*, *24*(2), 108–119. https://doi.org/10.1002/ppp.1779

Krogh, S. A., Pomeroy, J. W., & Marsh, P. (2017). Diagnosis of the hydrology of a small Arctic basin at the tundra-taiga transition using a physically based hydrological model. *Journal of Hydrology*, *550*, 685–703. https://doi.org/10.1016/j.jhydrol.2017.05.042

Ladson, A. R., Brown, R., Neal, B., & Nathan, R. (2013). A standard approach to baseflow separation using the Lyne and Hollick filter. *Australasian Journal of Water Resources*, *17*(1), 25–34. https://doi.org/10.7158/13241583.2013.11465417

Lafreniere, M. J., & Lamoureux, S. F. (2013). Thermal perturbation and rainfall runoff have greater impact on seasonal solute loads than physical disturbance of the active layer. *Permafrost and Periglacial Processes*, *24*(3), 241–251. https://doi.org/10.1002/ppp.1784

Lafrenière, M. J., & Lamoureux, S. F. (2019). Effects of changing permafrost conditions on hydrological processes and fluvial fluxes. *Earth-Science Reviews*, *191*, 212–223. https://doi.org/10.1016/j.earscirev.2019.02.018

Laudon, H., Spence, C., Buttle, J., Carey, S. K., McDonnell, J. J., McNamara, J. P., et al. (2017). Save northern high-latitude catchments. *Nature Geoscience*, *10*(5), 324–325. https://doi.org/10.1038/ngeo2947

Ledesma, J. L. J., Lupon, A., Martí, E., & Bernal, S. (2022). Hydrology and riparian forests drive carbon and nitrogen supply and DOC:NO3− stoichiometry along a headwater Mediterranean stream. *Hydrology and Earth System Sciences*, *26*(15), 4209–4232. https://doi.org/10.5194/hess-26-4209-2022

Letscher, R. T., Hansell, D. A., Kadko, D., & Bates, N. R. (2013). Dissolved organic nitrogen dynamics in the Arctic Ocean. *Marine Chemistry*, *148*, 1–9. https://doi.org/10.1016/j.marchem.2012.10.002

Levine, M. A., & Whalen, S. C. (2001). Nutrient limitation of phytoplankton production in Alaskan Arctic foothill lakes. *Hydrobiologia*, *455*(1), 189–201. https://doi.org/10.1023/A:1011954221491

Liu, X.-Y., Koba, K., Koyama, L. A., Hobbie, S. E., Weiss, M. S., Inagaki, Y., et al. (2018). Nitrate is an important nitrogen source for Arctic tundra plants. *Proceedings of the National Academy of Sciences*, *115*(13), 3398–3403. https://doi.org/10.1073/pnas.1715382115

Loranty, M. M., & Goetz, S. J. (2012). Shrub expansion and climate feedbacks in Arctic tundra. *Environmental Research Letters*, *7*(1), 011005. https://doi.org/10.1088/1748-9326/7/1/011005

MacIntyre, S., Sickman, J. O., Goldthwait, S. A., & Kling, G. W. (2006). Physical pathways of nutrient supply in a small, ultraoligotrophic arctic lake during summer stratification. *Limnology & Oceanography*, *51*(2), 1107–1124. https://doi.org/10.4319/lo.2006.51.2.1107

MacLean, R., Oswood, M. W., Irons, J. G., & McDowell, W. H. (1999). The effect of permafrost on stream biogeochemistry: A case study of two streams in the Alaskan (U.S.A.) taiga. *Biogeochemistry*, *47*(3), 239–267. https://doi.org/10.1007/BF00992909

Marcé, R., von Schiller, D., Aguilera, R., Martí, E., & Bernal, S. (2018). Contribution of hydrologic opportunity and biogeochemical reactivity to the variability of nutrient retention in river networks. *Global Biogeochemical Cycles*, *32*(3), 376–388. https://doi.org/10.1002/2017GB005677

McClelland, J. W., Stieglitz, M., Pan, F., Holmes, R. M., & Peterson, B. J. (2007). Recent changes in nitrate and dissolved organic carbon export from the upper Kuparuk River, North Slope, Alaska. *Journal of Geophysical Research*, *112*(G4). https://doi.org/10.1029/2006JG000371

McClelland, J. W., Townsend-Small, A., Holmes, R. M., Pan, F., Stieglitz, M., Khosh, M., & Peterson, B. J. (2014). River export of nutrients and organic matter from the North Slope of Alaska to the Beaufort Sea. *Water Resources Research*, *50*(2), 1823–1839. https://doi.org/10.1002/2013WR014722

McCrystall, M. R., Stroeve, J., Serreze, M., Forbes, B. C., & Screen, J. A. (2021). New climate models reveal faster and larger increases in Arctic precipitation than previously projected. *Nature Communications*, *12*(1). Article 1. https://doi.org/10.1038/s41467-021-27031-y

McGlynn, B. L., & McDonnell, J. J. (2003). Role of discrete landscape units in controlling catchment dissolved organic carbon dynamics. *Water Resources Research*, *39*(4). https://doi.org/10.1029/2002WR001525

McGuire, A. D., Lawrence, D. M., Koven, C., Clein, J. S., Burke, E., Chen, G., et al. (2018). Dependence of the evolution of carbon dynamics in the northern permafrost region on the trajectory of climate change. *Proceedings of the National Academy of Sciences of the United States of America*, *115*(15), 3882–3887. https://doi.org/10.1073/pnas.1719903115

McNamara, J. P., Kane, D. L., & Hinzman, L. D. (1998). An analysis of streamflow hydrology in the Kuparuk River basin, Arctic Alaska: A nested watershed approach. *Journal of Hydrology*, *206*(1–2), 39–57. https://doi.org/10.1016/S0022-1694(98)00083-3

McNamara, J. P., Kane, D. L., Hobbie, J. E., & Kling, G. W. (2008). Hydrologic and biogeochemical controls on the spatial and temporal patterns of nitrogen and phosphorus in the Kuparuk River, arctic Alaska. *Hydrological Processes*, *22*(17), 3294–3309. https://doi.org/10.1002/hyp.6920

Mevik, B.-H., & Wehrens, R. (2007). The pls Package: Principal component and partial least squares regression in R. *Journal of Statistical Software*, *18*(1), 1–23. https://doi.org/10.18637/jss.v018.i02

Moatar, F., Abbott, B. W., Minaudo, C., Curie, F., & Pinay, G. (2017). Elemental properties, hydrology, and biology interact to shape concentration-discharge curves for carbon, nutrients, sediment, and major ions. *Water Resources Research*, *53*(2), 1270–1287. https://doi.org/10.1002/2016WR019635

Musolff, A., Fleckenstein, J. H., Opitz, M., Büttner, O., Kumar, R., & Tittel, J. (2018). Spatio-temporal controls of dissolved organic carbon stream water concentrations. *Journal of Hydrology*, *566*, 205–215. https://doi.org/10.1016/j.jhydrol.2018.09.011

Musolff, A., Selle, B., Büttner, O., Opitz, M., & Tittel, J. (2017). Unexpected release of phosphate and organic carbon to streams linked to declining nitrogen depositions. *Global Change Biology*, *23*(5), 1891–1901. https://doi.org/10.1111/gcb.13498

Myers-Smith, I. H., Forbes, B. C., Wilmking, M., Hallinger, M., Lantz, T., Blok, D., et al. (2011). Shrub expansion in tundra ecosystems: Dynamics, impacts and research priorities. *Environmental Research Letters*, *6*(4), 045509. https://doi.org/10.1088/1748-9326/6/4/045509

Neff, J. C., Chapin, F. S., III., & Vitousek, P. M. (2003). Breaks in the cycle: Dissolved organic nitrogen in terrestrial ecosystems. *Frontiers in Ecology and the Environment*, *1*(4), 205–211. https://doi.org/10.1890/1540-9295(2003)001[0205:BITCDO]2.0.CO;2

Neilson, B. T., Cardenas, M. B., O'Connor, M. T., Rasmussen, M. T., King, T. V., & Kling, G. W. (2018). Groundwater flow and exchange across the land surface explain carbon export patterns in continuous permafrost watersheds. *Geophysical Research Letters*, *45*(15), 7596–7605. https://doi.org/10.1029/2018GL078140

Paquette, M., Fortier, D., & Vincent, W. F. (2018). Hillslope water tracks in the High Arctic: Seasonal flow dynamics with changing water sources in preferential flow paths. *Hydrological Processes*, *32*(8), 1077–1089. https://doi.org/10.1002/hyp.11483

Pastor, A., Poblador, S., Skovsholt, L. J., & Riis, T. (2020). Microbial carbon and nitrogen processes in high-Arctic riparian soils. *Permafrost and Periglacial Processes*, *31*(1), 223–236. https://doi.org/10.1002/ppp.2039

Paulsen, M. L., Seuthe, L., Reigstad, M., Larsen, A., Cape, M. R., & Vernet, M. (2018). Asynchronous accumulation of organic carbon and nitrogen in the Atlantic Gateway to the Arctic Ocean. *Frontiers in Marine Science*, *5*, 1–17. https://www.frontiersin.org/articles/10.3389/fmars.2018.00416

Pellerin, B. A., Stauffer, B. A., Young, D. A., Sullivan, D. J., Bricker, S. B., Walbridge, M. R., et al. (2016). Emerging tools for continuous nutrient monitoring networks: Sensors advancing science and water resources protection. *JAWRA Journal of the American Water Resources Association*, *52*(4), 993–1008. https://doi.org/10.1111/1752-1688.12386

Perumal, M., Moramarco, T., Sahoo, B., & Barbetta, S. (2007). A methodology for discharge estimation and rating curve development at ungauged river sites. *Water Resources Research*, *43*(2). https://doi.org/10.1029/2005WR004609

Plont, S., O'Donnell, B. M., Gallagher, M. T., & Hotchkiss, E. R. (2020). Linking carbon and nitrogen spiraling in streams. *Freshwater Science*, *39*(1), 126–136. https://doi.org/10.1086/707810

Prowse, T., Bring, A., Mård, J., Carmack, E., Holland, M., Instanes, A., et al. (2015). Arctic freshwater synthesis: Summary of key emerging issues. *Journal of Geophysical Research: Biogeosciences*, *120*(10), 1887–1893. https://doi.org/10.1002/2015JG003128

R Core Team. (2014). R: A language and environment for statistical computing. *R Core Team*, *3*(1), 201.

Raymond, P. A., & Saiers, J. E. (2010). Event controlled DOC export from forested watersheds. *Biogeochemistry*, *100*(1–3), 197–209. https://doi.org/10.1007/s10533-010-9416-7

Raymond, P. A., Saiers, J. E., & Sobczak, W. V. (2016). Hydrological and biogeochemical controls on watershed dissolved organic matter transport: Pulse-shunt concept. *Ecology*, *97*(1), 5–16. https://doi.org/10.1890/14-1684.1

Rode, M., Wade, A. J., Cohen, M. J., Hensley, R. T., Bowes, M. J., Kirchner, J. W., et al. (2016). Sensors in the stream: The high-frequency wave of the present. *Environmental Science & Technology*, *50*(19), 10297–10307. https://doi.org/10.1021/acs.est.6b02155

Rodríguez-Cardona, B. M., Coble, A. A., Wymore, A. S., Kolosov, R., Podgorski, D. C., Zito, P., et al. (2020). Wildfires lead to decreased carbon and increased nitrogen concentrations in upland arctic streams. *Scientific Reports*, *10*(1). Article 1. https://doi.org/10.1038/s41598-020-65520-0

Rose, L. A., Karwan, D. L., & Godsey, S. E. (2018). Concentration-discharge relationships describe solute and sediment mobilization, reaction, and transport at event and longer timescales. *Hydrological Processes*, *32*(18), 2829–2844. https://doi.org/10.1002/hyp.13235

Ruhala, S. S., & Zarnetske, J. P. (2017). Using in-situ optical sensors to study dissolved organic carbon dynamics of streams and watersheds: A review. *Science of the Total Environment*, *575*, 713–723. https://doi.org/10.1016/j.scitotenv.2016.09.113

Sakamoto, C. M., Johnson, K. S., & Coletti, L. J. (2009). Improved algorithm for the computation of nitrate concentrations in seawater using an in situ ultraviolet spectrophotometer. *Limnology and Oceanography: Methods*, *7*(1), 132–143. https://doi.org/10.4319/lom.2009.7.132

Saros, J. E., Arp, C. D., Bouchard, F., Comte, J., Couture, R.-M., Dean, J. F., et al. (2022). Sentinel responses of Arctic freshwater systems to climate: Linkages, evidence, and a roadmap for future research. *Arctic Science*, *9*(2), 356–392. https://doi.org/10.1139/as-2022-0021

Schuur, E. A. G., Abbott, B. W., Commane, R., Ernakovich, J., Euskirchen, E., Hugelius, G., et al. (2022). Permafrost and climate change: Carbon cycle feedbacks from the warming Arctic. *Annual Review of Environment and Resources*, *47*(1), 343–371. https://doi.org/10.1146/annurev-environ-012220-011847

Shogren, A., Zarnetske, J., Bowden, W., & Abbott, B. (2023a). High-frequency dissolved organic carbon, nitrate, and total dissolved nitrogen from the Oksrukuyik Creek outlet near Toolik Field Station, Alaska, summer 2020-2021 [Dataset]. Arctic Data Center. https://doi.org/10.18739/A2MG7FX54

Shogren, A., Zarnetske, J., Bowden, W., & Abbott, B. (2023b). High-frequency dissolved organic carbon, nitrate, and total dissolved nitrogen from the Kuparuk River outlet near Toolik Field Station, Alaska, summer 2020-2021 [Dataset]. Arctic Data Center. https://doi.org/10.18739/A2GQ6R40X

Shogren, A. J., Zarnetske, J. P., Abbott, B. W., Bratsman, S., Brown, B., Carey, M. P., et al. (2022). Multi-year, spatially extensive, watershed-scale synoptic stream chemistry and water quality conditions for six permafrost-underlain Arctic watersheds. *Earth System Science Data*, *14*(1), 95–116. https://doi.org/10.5194/essd-14-95-2022

Shogren, A. J., Zarnetske, J. P., Abbott, B. W., Iannucci, F., & Bowden, W. B. (2020). We cannot shrug off the shoulder seasons: Addressing knowledge and data gaps in an Arctic Headwater. *Environmental Research Letters*, *15*, 104027. https://doi.org/10.1088/1748-9326/ab9d3c

Shogren, A. J., Zarnetske, J. P., Abbott, B. W., Iannucci, F., Frei, R. J., Griffin, N. A., & Bowden, W. B. (2019). Revealing biogeochemical signatures of Arctic landscapes with river chemistry. *Scientific Reports*, *9*(1), 1–11. https://doi.org/10.1038/s41598-019-49296-6

Shogren, A. J., Zarnetske, J. P., Abbott, B. W., Iannucci, F., Medvedeff, A., Cairns, S., et al. (2021). Arctic concentration–discharge relationships for dissolved organic carbon and nitrate vary with landscape and season. *Limnology & Oceanography*, *66*(1), S197–S215. https://doi.org/10.1002/lno.11682

Starr, S., Johnston, S. E., Sobolev, N., Perminova, I., Kellerman, A., Fiske, G., et al. (2023). Characterizing uncertainty in Pan-Arctic land-ocean dissolved organic carbon flux: Insights from the Onega River, Russia. *Journal of Geophysical Research: Biogeosciences*, *128*(5), e2022JG007073. https://doi.org/10.1029/2022JG007073

Tank, S. E., Manizza, M., Holmes, R. M., McClelland, J. W., & Peterson, B. J. (2012). The processing and impact of dissolved riverine nitrogen in the Arctic Ocean. *Estuaries and Coasts*, *35*(2), 401–415. https://doi.org/10.1007/s12237-011-9417-3

Tank, S. E., McClelland, J. W., Spencer, R. G. M., Shiklomanov, A. I., Suslova, A., Moatar, F., et al. (2023). Recent trends in the chemistry of major northern rivers signal widespread Arctic change. *Nature Geoscience*, *16*(9). Article 9. https://doi.org/10.1038/s41561-023-01247-7

Tank, S. E., Vonk, J. E., Walvoord, M. A., McClelland, J. W., Laurion, I., & Abbott, B. W. (2020). Landscape matters: Predicting the biogeochemical effects of permafrost thaw on aquatic networks with a state factor approach. *Permafrost and Periglacial Processes*, 1–13. https://doi.org/10.1002/ppp.2057

Taylor, P. G., & Townsend, A. R. (2010). Stoichiometric control of organic carbon–nitrate relationships from soils to the sea. *Nature*, *464*(7292). Article 7292. https://doi.org/10.1038/nature08985

Thompson, S. E., Basu, N. B., Lascurain, J., Aubeneau, A., & Rao, P. S. C. (2011). Relative dominance of hydrologic versus biogeochemical factors on solute export across impact gradients. *Water Resources Research*, *47*(10). https://doi.org/10.1029/2010WR009605

Townsend-Small, A., McClelland, J. W., Max Holmes, R., & Peterson, B. J. (2011). Seasonal and hydrologic drivers of dissolved organic matter and nutrients in the upper Kuparuk River, Alaskan Arctic. *Biogeochemistry*, *103*(1–3), 109–124. https://doi.org/10.1007/s10533-010-9451-4

Treharne, R., Rogers, B. M., Gasser, T., MacDonald, E., & Natali, S. (2022). Identifying barriers to estimating carbon release from interacting feedbacks in a warming Arctic. *Frontiers in Climate*, *3*. https://www.frontiersin.org/articles/10.3389/fclim.2021.716464

Turnipseed, D. P., & Sauer, V. B. (2010). *Discharge measurements at gaging stations* (USGS Numbered series 3-A8; Techniques and methods). U.S. Geological Survey. Retrieved from http://pubs.er.usgs.gov/publication/tm3A8

Vaughan, M. C. H., Bowden, W. B., Shanley, J. B., Vermilyea, A., Sleeper, R., Gold, A. J., et al. (2017). High-frequency dissolved organic carbon and nitrate measurements reveal differences in storm hysteresis and loading in relation to land cover and seasonality. *Water Resources Research*, *53*(7), 5345–5363. https://doi.org/10.1002/2017WR020491

Vaughan, M. C. H., Bowden, W. B., Shanley, J. B., Vermilyea, A., Wemple, B., & Schroth, A. W. (2018). Using in situ UV-Visible spectrophotometer sensors to quantify riverine phosphorus partitioning and concentration at a high frequency. *Limnology and Oceanography: Methods*, *16*(12), 840–855. https://doi.org/10.1002/lom3.10287

Virkkala, A.-M., Abdi, A. M., Luoto, M., & Metcalfe, D. B. (2019). Identifying multidisciplinary research gaps across Arctic terrestrial gradients. *Environmental Research Letters*, *14*(12), 124061. https://doi.org/10.1088/1748-9326/ab4291

Vonk, J. E., Speetjens, N. J., & Poste, A. E. (2023). Small watersheds may play a disproportionate role in arctic land-ocean fluxes. *Nature Communications*, *14*(1). Article 1. https://doi.org/10.1038/s41467-023-39209-7

Vonk, J. E., Tank, S. E., Bowden, W. B., Laurion, I., Vincent, W. F., Alekseychik, P., et al. (2015). Reviews and syntheses: Effects of permafrost thaw on Arctic aquatic ecosystems. *Biogeosciences*, *12*(23), 7129–7167. https://doi.org/10.5194/bg-12-7129-2015

Vonk, J. E., Tank, S. E., & Walvoord, M. A. (2019). Integrating hydrology and biogeochemistry across frozen landscapes. *Nature Communications*, *10*(1), 1–4. https://doi.org/10.1038/s41467-019-13361-5

Voytek, E. B., Rushlow, C. R., Godsey, S. E., & Singha, K. (2016). Identifying hydrologic flowpaths on arctic hillslopes using electrical resistivity and self potential. *Geophysics*, *81*(1), WA225–WA232. https://doi.org/10.1190/geo2015-0172.1

Wagner, S., Fair, J. H., Matt, S., Hosen, J. D., Raymond, P., Saiers, J., et al. (2019). Molecular hysteresis: Hydrologically driven changes in riverine dissolved organic matter chemistry during a storm event. *Journal of Geophysical Research: Biogeosciences*, *124*(4), 759–774. https://doi.org/10.1029/2018JG004817

Walker, D. A., & Maier, H. A. (2008). *Vegetation in the vicinity of the Toolik field station*. Alaska [Technical Report]. University of Alaska. Institute of Arctic Biology. Retrieved from https://scholarworks.alaska.edu/handle/11122/1557

Walker, D. A., & Raynolds, M. K. (2017). Maps of Vegetation Types and Physiographic Features, Kuparuk River Basin, Alaska. *ORNL DAAC*. https://doi.org/10.3334/ORNLDAAC/1378

Walvoord, M. A., & Kurylyk, B. L. (2016). Hydrologic impacts of thawing permafrost—A review. *Vadose Zone Journal*, *15*(6). https://doi.org/10.2136/vzj2016.01.0010

Webster, A. J., Douglas, T. A., Regier, P., Scheuerell, M. D., & Harms, T. K. (2021). Multi-scale temporal patterns in stream biogeochemistry indicate linked permafrost and ecological dynamics of boreal catchments. *Ecosystems*. https://doi.org/10.1007/s10021-021-00709-6

Weiler, M., & McDonnell, J. J. (2006). Testing nutrient flushing hypotheses at the hillslope scale: A virtual experiment approach. *Journal of Hydrology*, *319*(1), 339–356. https://doi.org/10.1016/j.jhydrol.2005.06.040

Wickland, K. P., Waldrop, M. P., Aiken, G. R., Koch, J. C., Jorgenson, M. T., & Striegl, R. G. (2018). Dissolved organic carbon and nitrogen release from boreal Holocene permafrost and seasonally frozen soils of Alaska. *Environmental Research Letters*, *13*(6), 065011. https://doi.org/10.1088/1748-9326/aac4ad

Wollheim, W. M., Bernal, S., Burns, D. A., Czuba, J. A., Driscoll, C. T., Hansen, A. T., et al. (2018). River network saturation concept: Factors influencing the balance of biogeochemical supply and demand of river networks. *Biogeochemistry*, *141*(3), 503–521. https://doi.org/10.1007/s10533-018-0488-0

Wymore, A. S., Fazekas, H. M., & McDowell, W. H. (2021). Quantifying the frequency of synchronous carbon and nitrogen export to the river network. *Biogeochemistry*, *152*(1), 1–12. https://doi.org/10.1007/s10533-020-00741-z

Zarnetske, J. P., Bowden, W. B., Abbott, B. W., & Shogren, A. J. (2020a). High-frequency dissolved organic carbon and nitrate from the Kuparuk River outlet near Toolik Field Station, Alaska, summer 2017–2019 [Dataset]. EDI Data Portal. https://doi.org/10.6073/pasta/990958760c13cdd55b574c5202dc19b7

Zarnetske, J. P., Bowden, W. B., Abbott, B. W., & Shogren, A. J. (2020b). High-frequency dissolved organic carbon and nitrate from the Oksrukuyik Creek outlet near Toolik Field Station, Alaska, summer 2017–2019 [Dataset]. EDI Data Portal. https://doi.org/10.6073/pasta/5d63c098887205597ce0df929467168c

Zarnetske, J. P., Bowden, W. B., Abbott, B. W., & Shogren, A. J. (2020c). High-frequency dissolved organic carbon and nitrate from the Trevor Creek outlet near Toolik Field Station, Alaska, summer 2017–2019 [Dataset]. EDI Data Portal. https://doi.org/10.6073/pasta/3bd6a1d2d9487546f32d46d2943c6e43

Zarnetske, J. P., Bouda, M., Abbott, B. W., Saiers, J., & Raymond, P. A. (2018). Generality of hydrologic transport limitation of watershed organic carbon flux across ecoregions of the United States. *Geophysical Research Letters*, *45*, 11702–11711. https://doi.org/10.1029/2018GL080005

Zimmer, M. A., Pellerin, B., Burns, D. A., & Petrochenkov, G. (2019). Temporal variability in nitrate-discharge relationships in large rivers as revealed by high-frequency data. *Water Resources Research*, *55*(2), 973–989. https://doi.org/10.1029/2018WR023478